

Bayesian spatial+: A joint model perspective

Isa Marques¹

Paul F.V. Wiemann^{1,2}

imarques@uni-goettingen.de

¹ Georg-August-University of Göttingen, Chairs of Statistics and Econometrics, Humboldtallee 3,
37073 Göttingen, Germany

² Texas A&M University, Department of Statistics, College Station, TX, USA

Abstract

A common phenomenon in spatial regression models is spatial confounding. This phenomenon occurs when spatially indexed covariates modeling the mean of the response are correlated with a spatial effect included in the model. `spatial+` (Dupont et al., 2022) is a popular approach to reducing spatial confounding. `spatial+` is a two-stage frequentist approach that explicitly models the spatial structure in the confounded covariate, removes it, and uses the corresponding residuals in the second stage. In a frequentist setting, there is no uncertainty propagation from the first stage estimation determining the residuals since only point estimates are used. Inference can also be cumbersome in a frequentist setting, and some of the gaps in the original approach can easily be remedied in a Bayesian framework. First, a Bayesian joint model can easily achieve uncertainty propagation from the first to the second stage of the model. In a Bayesian framework, we also have the tools to infer the model’s parameters directly. Notably, another advantage of using a Bayesian framework we thoroughly explore is the ability to use prior information to impose restrictions on the spatial effects rather than applying them directly to their posterior. We build a joint prior for the smoothness of all spatial effects that simultaneously shrinks towards a high smoothness of

the response and imposes that the spatial effect in the response is a smoother of the confounded covariates' spatial effect. This prevents the response from operating at a smaller scale than the covariate and can help to avoid situations where there is insufficient variation in the residuals resulting from the first stage model. We evaluate the performance of the Bayesian spatial+ via both simulated and real datasets.

1 Introduction

Spatial regression models are traditionally used when there is residual spatial dependence in a regression model after accounting for observed covariates. Residual spatial dependence can be thought of as the result of unobserved, spatially varying covariates. If these unobserved covariates are correlated with the observed covariates, the regression coefficients associated with the latter may be biased and their uncertainty may be underestimated. A common approach considered to adjust for unobserved spatial covariates is to approximate their overall effect by a given unknown function $f(\cdot)$ defined on the spatial domain.

Consider $y(\mathbf{s}_i)$ is observed within the spatial domain \mathcal{S} at location $\mathbf{s}_i \in \mathcal{S} \subseteq \mathbb{R}^2$, for $i = 1, \dots, n$ and it can be modeled as

$$y(\mathbf{s}_i) = \beta_0 + \mathbf{x}^{obs}(\mathbf{s}_i)' \boldsymbol{\beta}_{obs} + f(\mathbf{s}_i) + \varepsilon_i \quad (1)$$

where $\mathbf{x}^{obs}(\mathbf{s}) = (x_1^{obs}(\mathbf{s}), \dots, x_{p_{obs}}^{obs}(\mathbf{s}))'$ are observed covariates, $\boldsymbol{\varepsilon} = (\varepsilon_1, \dots, \varepsilon_n)'$ is the vector of errors with mean $\mathbf{0}$ and variance-covariance matrix $\sigma^2 \mathbf{I}$, and $\boldsymbol{\beta} = (\beta_0, \boldsymbol{\beta}_{obs}')'$ are unknown coefficients. The function $f(\cdot)$ approximates unobserved spatial variation such that $f(\mathbf{s}) \approx \mathbf{x}^{unobs}(\mathbf{s})' \boldsymbol{\beta}_{unobs}$, where $\mathbf{x}^{unobs}(\mathbf{s}) = (x_1^{unobs}(\mathbf{s}), \dots, x_{p_{unobs}}^{unobs}(\mathbf{s}))'$ is a vector of unobserved covariates relevant to explain the response.

Potential spatial dependence between observed and unobserved covariates tends to be carried over to the spatial dependence between $f(\mathbf{s})$ and $\mathbf{x}^{obs}(\mathbf{s})$ in Equation (1), and aggravated by smoothing (Dupont et al., 2022), with the consequence that the estimates of the

regression coefficients are biased and the corresponding standard errors inflated. Thus, spatial confounding becomes relevant to various areas of science where the interpretation of the regression coefficients in spatial regression models are of interest, such as forestry, ecology, epidemiology, among many others. Clayton et al. (1993) first identified this phenomenon, which was latter named “spatial confounding” by Reich et al. (2006), but it has been more recently that spatial confounding has become a popular topic, with multiple articles discussing its sources and potential remedies (e.g. Reich et al., 2006; Paciorek, 2010; Thaden and Kneib, 2018; Khan and Calder, 2020; Dupont et al., 2022; Marques et al., 2022; Guan et al., 2022).

The first papers discussing how to remedy spatial confounding proposed restricted spatial regression (RSR) as a solution (Reich et al., 2006; Hanks et al., 2015). At the same time results by Khan and Calder (2020), an later Zimmerman and Ver Hoef (2021), showed that RSR might behave worse than non-spatial models in terms of the coverage of the associated regression coefficients, multiple new methods emerged that aim at reducing spatial confounding (Thaden and Kneib, 2018; Dupont et al., 2022; Marques et al., 2022; Guan et al., 2022; Schnell and Papadogeorgou, 2020). When it comes to the sources of spatial confounding itself, the spatial scales of both the observed covariate and the spatial effect $f(\cdot)$ are considered a critical identifying factor of spatial confounding (Paciorek, 2010; Guan et al., 2022; Mäkinen et al., 2022), which is rarely disputed (Khan and Berrett, 2023).

One of the latest developments for mitigating spatial confounding that received much attention due to its straightforward interpretation and implementability is spatial+ (Dupont et al., 2022). This is demonstrated by the several related research and discussion papers (Marques and Kneib, 2022; Reich et al., 2022; Urdangarin et al., 2022; Khan and Berrett, 2023; Urdangarin et al., 2023). The spatial+ method is based on a two-stage frequentist model where on the first stage a spatial model is fit to the confounded covariate and in the second-stage the same confounded covariate is replaced by the corresponding residuals from the first-stage. Thus, by modeling away the spatial structure in each $\mathbf{x}^{obs}(\mathbf{s})$, there should

be less confounding at the response’s level.

In this paper, we bring spatial+ to the Bayesian framework. The Bayesian approach is beneficial for several reasons, most notably: (1) uncertainty quantification (UQ) works well in a Bayesian joint model, where the two stages of the model can be estimated simultaneously, thus accounting for uncertainty propagation from the first to the second stage, (2) the Bayesian paradigm allows straightforward inference about the model’s parameters compared to a frequentist approach and thus can remedy some of its limitations, and (3) one can impose restrictions on the prior rather than the posterior distribution (in contrast to e.g., RSR) and include in the prior knowledge about the sources of spatial confounding, such as the spatial scale. Concretely, we propose a joint prior for smoothness based on the idea that when the spatial effect operates on a smaller scale than the observed covariate, it is likely to explain the data better than the covariate (Paciorek, 2010; Marques et al., 2022; Mäkinen et al., 2022). Hence, our prior prevents the spatial scale of the spatial effect $f(\cdot)$ from being smaller than the observed covariate’s and can prevent the residuals on the first stage from having too little variability.

The set-ups we focus on, are those where the interpretation of the effects $\mathbf{x}^{obs}(\mathbf{s})'\boldsymbol{\beta}_{obs}$ is of primary interest, and we analyze not only the bias of the estimated $\boldsymbol{\beta}_{obs}$ but also the corresponding UQ which is relevant, e.g., to obtain coverage rates. While similar point estimates result from either frequentist or Bayesian models, a joint model has the distinct advantage of integrating all steps in one joint estimation problem such that estimates of uncertainty will in general differ. Should the predictive power of the model be the main concern, there is thus far limited literature (Page et al., 2017), which indicates that the predictions might improve under spatial confounding.

The paper is organized as follows. Section 2 briefly reviews spatial+ from Dupont et al. (2022). Section 3 introduces the Bayesian spatial+ model, including the proposed joint Bayesian estimation and the joint prior on smoothness of all spatial effects. Section 4 briefly discusses extensions to the model to multiple covariates. In Section 5, the performance

of the model is evaluated in three extensive simulations where we compare our model to the frequentist counterparts. In Section 6 we consider two applications: First, we study meteorological data in Germany, namely daily average precipitation. Second, we revisit the forest cover example in Dupont et al. (2022).

2 A brief review of frequentist spatial+

Consider a single observed covariate $x_{obs}(\cdot)$. For the sake of notational simplicity, we drop *obs* as a index. Our starting point is the adjusted spatial model as in Dupont et al. (2022). spatial+ is a two-stage regression model:

$$x(\mathbf{s}_i) = \beta_0^x + f^x(\mathbf{s}_i) + \varepsilon_i^x, \quad (2a)$$

$$y(\mathbf{s}_i) = \beta_0 + \beta(x(\mathbf{s}_i) - \hat{g}^x(\mathbf{s}_i)) + f(\mathbf{s}_i) + \varepsilon_i \quad (2b)$$

where $f(\cdot)$ and $f^x(\cdot)$ are smooth functions defined on the spatial domain $\mathcal{S} \subseteq \mathbb{R}^2$, and $\varepsilon_i^x \sim N(0, \sigma_x^2)$ and $\varepsilon_i \sim N(0, \sigma^2)$ are *i.i.d* random errors. \hat{g}^x is defined as $\hat{g}^x(\mathbf{s}) = \hat{\beta}_0^x + \hat{f}^x(\mathbf{s})$, where $\hat{\beta}_0^x$ and $\hat{f}^x(\mathbf{s})$ are the fitted values of β_0^x and $f^x(\mathbf{s})$ from Equation (2a), respectively.

Hence, the model implies: (1) the spatial structure in $x(\mathbf{s}_i)$ as captured by $f^x(\mathbf{s}_i)$ is removed from the covariate $x(\mathbf{s}_i)$ and on the second stage ε_i^x is used to identify β , (2) uncertainty arising from the first stage estimation is unaccounted for on the second stage, (3) the model requires the separability of $f^x(\mathbf{s}_i)$ and ε_i^x . We will mostly focus on (1) and (2) throughout the paper, while (3) is an essential feature of Dupont et al. (2022), which, e.g., complicates extensions to non-Gaussian covariates, but it is also part of the simplicity of the concept that makes it attractive and understandable for a broad audience.

2.1 Approximating $f(\cdot)$

A popular way of approximating $f(\cdot)$ is using bivariate basis functions approaches (Ramsay, 2002; Wood, 2003; Sangalli et al., 2013; Ugarte et al., 2017). We approximate it with a linear combination of basis functions evaluated at each observed location $\mathbf{s}_j \in \mathcal{S}$:

$$f(\mathbf{s}) = \sum_{j=1}^d \gamma_j B(\mathbf{s}_j).$$

Similar, for $f^x(\cdot)$. For computationally purposes, ideally $d < n$, which can be attained by using, e.g., thin plate regression splines (TPRS) (Wood, 2003).

In the case of the two-stage model in Equations (2a) and (2b), spline smoothers $f^x(\cdot)$ and $f(\cdot)$ over a 2-dimensional surface can be defined as the solution that minimizes each of the following two penalized sum of squares, respectively:

$$\sum_{i=1}^n (x(\mathbf{s}_i) - (\beta_0^x + f^x(\mathbf{s}_i)))^2 + \lambda_x J(f^x) \quad (3a)$$

$$\sum_{i=1}^n (y(\mathbf{s}_i) - (\beta_0 + \beta \hat{\varepsilon}_i^x + f(\mathbf{s}_i)))^2 + \lambda J(f). \quad (3b)$$

The penalty terms $J(f)$ and $J(f^x)$ can be, e.g., the bivariate analogue of the integrated squared second derivative and the smoothing parameters $\lambda_x, \lambda > 0$ govern the contribution of the penalties to inference.

In matrix notation, write $\hat{\mathcal{E}}^x = (1, \hat{\varepsilon}^x)$ where $\hat{\varepsilon}^x = (\hat{\varepsilon}_1^x, \dots, \hat{\varepsilon}_n^x)'$, $\hat{\varepsilon} = (\hat{\varepsilon}_1, \dots, \hat{\varepsilon}_n)'$, $\beta = (\beta_0, \beta)'$, $Z[i, j] = B(\mathbf{s}_j)$, $\gamma = (\gamma_1, \dots, \gamma_d)'$, $\gamma^x = (\gamma_1^x, \dots, \gamma_d^x)'$, $\mathbf{y} = (y_1, \dots, y_n)'$. Then, Equation (2b) can be expressed as

$$\mathbf{x} = \beta_0^x \mathbf{1} + \mathbf{Z} \gamma^x + \boldsymbol{\varepsilon}^x, \quad (4a)$$

$$\mathbf{y} = \hat{\mathcal{E}}^x \beta + \mathbf{Z} \gamma + \boldsymbol{\varepsilon}. \quad (4b)$$

It can be shown that the penalties $J(f^x)$ and $J(f)$ can equivalently be represented as

$$\gamma' \mathbf{K} \gamma \quad \text{and} \quad \gamma^{x'} \mathbf{K} \gamma^x.$$

where \mathbf{K} are potentially rank deficient penalty matrices. The potential rank deficiency of \mathbf{K} becomes relevant in Section 3.3 when building priors for the Bayesian spatial+.

The theory in Dupont et al. (2022) was developed for partial thin plate spline models (Engle et al., 1986; Wahba, 1984) and tested using TPRS. Throughout this paper, for computational purposes, we also focus on TPRS, which are low rank approximations to thin plate splines. The full rank thin plate splines are derived from a set of radial basis functions, and TPRSs achieve computational benefits by using a truncated eigenbasis to approximate the radial basis. However, as indicated in this section, the same concept should be applicable to other basis functions approaches or Gaussian and Gaussian Markov random fields approaches.

2.2 Relevant properties of the frequentist spatial+

Dupont et al. (2022) show that a standard unadjusted spatial model such as in Equation (1) without the smoothing penalty is an ordinary linear model in which all effect estimates are unbiased. Thus, in a spatial model that does not adjust for confounding, we cannot avoid potential excessive bias in $\hat{\beta}$ unless the smooth term is undersmoothed.

In the specific case of spatial+, however, Dupont et al. (2022) show that $\hat{\beta}$ is root-n consistent and when the parameters λ_x and λ converge at the optimal rate that minimizes the average mean squared error of the estimated spatial effect, the bias of the covariate effect estimate $\hat{\beta}$ converges to 0 faster than the standard deviation and, therefore, does not become disproportionately large. Concretely, the optimal rate of $\lambda\lambda_x = o(n^{-1})$ ensures that the bias of the spatial+ estimate converges faster than the standard deviation of the estimate. Thus, the authors also show that unlike the standard spatial model's estimate for $\hat{\beta}$, the spatial+'s

estimates do not need undersmoothing to avoid excessive bias. We will use this idea when building priors for the Bayesian spatial+ in Section 3, while the convergence conditions are tested in a simulation study in a Bayesian framework.

One relevant aspect concerning the frequentist spatial+ and UQ, in particular, is that it is not discussed whether resampling approaches, such as bootstrap work to estimate its variance and conduct inference on β (Reich et al., 2022). We believe Bayesian inference can provide a easy remedy to the potential difficulties in doing inference for the frequentist spatial+.

3 Bayesian spatial+

3.1 Bayesian joint modeling and uncertainty quantification

We reconsider spatial+ in a Bayesian framework, using Markov chain Monte Carlo (MCMC). This has three significant advantages over the frequentist spatial+ in Section 2.

Firstly, by considering a joint MCMC scheme one can easily replace $\hat{g}^x(\mathbf{s}_i) = \hat{\beta}_0^x + \hat{f}^x(\mathbf{s}_i)$ in Equation (2b), by $g^x(\mathbf{s}_i) = \beta_0^x + f^x(\mathbf{s}_i)$. In contrast, one well-known limitation of traditional sequential methods is that they potentially misstate the uncertainty in causal estimates by treating the estimated as a known quantity in the response stage (Gelman and Hill, 2006). While similar point estimates will result from fitting separate MCMC schemes for the first and second stage, the UQ about the model parameters can change considerably, as the quality of the fit of the model on the first stage will be reflected on the second stage.

Secondly, another significant advantage of employing a Bayesian framework, as opposed to a frequentist approach, in uncertainty quantification is the ability to obtain posterior distributions for each unknown parameter. The Bayesian approach acknowledges that uncertainty is an inherent part of the modeling process and instead of providing point estimates, Bayesian inference provides a probability distribution over the parameter space. Through MCMC sampling, we obtain a set of samples from the posterior distribution, allowing us

to summarize uncertainty in various ways, such as credible intervals. Thus, we can explore the entire range of plausible parameter values, capturing the uncertainty associated with our estimates.

It is important to note that the reliability of the uncertainty estimates heavily relies on the convergence of the MCMC algorithm. Convergence ensures that the sampled values adequately explore the posterior distribution, allowing for accurate inference. Diagnostic tools, such as trace plots and the R-hat statistic (Gelman et al., 1992; Vehtari et al., 2021), are employed to assess the convergence of the MCMC chains.

Finally, in a Bayesian framework, one can impose restrictions on the prior rather than directly on the posterior distribution, e.g., as in RSR, which we consider to be less problematic as, ultimately, if the data favors a different behavior, the prior will be weighted out with increasing sample size, although its support must still be respected to avoid full conditionals of 0.

3.2 Model structure

Our starting point is now a spatial model formulated as in Equations (2a) and (2b), where $\hat{g}^x(\mathbf{s}_i)$ is replaced by $g^x(\mathbf{s}_i) = \beta_0^x + f^x(\mathbf{s}_i)$, and so we use $\varepsilon^x = x(\mathbf{s}) - g^x(\mathbf{s})$ in the response model. In matrix notation, we consider now $\boldsymbol{\varepsilon}^x = (1, \boldsymbol{\varepsilon}^x)$ where $\boldsymbol{\varepsilon}^x = (\varepsilon_1^x, \dots, \varepsilon_n^x)'$.

Let $r = \text{rk}(\mathbf{K}) \leq d$ denote the rank of the penalty matrix and $d = \dim(\boldsymbol{\gamma})$ the dimension of the coefficient vectors. If $\lambda = \sigma^2/\tau^2$ (Nychka, 2000), the objective function in Equation (3a) is proportional to the log-posterior density of $\boldsymbol{\gamma}$, given the partially improper prior with density function

$$\boldsymbol{\gamma}|\tau^2 \propto (\tau^2)^{-r/2} \exp\left(-\frac{1}{2\tau^2}\boldsymbol{\gamma}'\mathbf{K}\boldsymbol{\gamma}\right). \quad (5)$$

The Gaussian likelihood for \mathbf{y} is

$$\mathbf{y}|\boldsymbol{\gamma}, \sigma^2, \mathbf{x} \sim N(\boldsymbol{\varepsilon}^x\boldsymbol{\beta} + \mathbf{Z}\boldsymbol{\gamma}, \sigma^2\mathbf{I}). \quad (6)$$

Hence, apparently, τ^2 controls the smoothness of the function $f(\cdot)$.

However, in this direct approach, we encounter the problem that the inverse of \mathbf{K} generally does not exist, since the penalty \mathbf{K} may not have full rank. Due to the potential rank deficiency, the null space of the precision matrix \mathbf{K} will in some cases be non-trivial. In order to deal with the impropriety of Equation (5), we split γ into two subvectors γ_{pen} and γ_{unpen} with dimensionalities depending on the rank deficiency of \mathbf{K} . We consider the re-parametrization

$$\gamma = \tilde{\mathbf{V}}\gamma_{pen} + \tilde{\mathbf{U}}\gamma_{unpen} \quad (7)$$

where $d \times (d-r)$ and $d \times r$ dimensional matrices $\tilde{\mathbf{V}}$ and $\tilde{\mathbf{U}}$, respectively, such that $\tilde{\mathbf{V}}'\mathbf{K}\tilde{\mathbf{V}} = \mathbf{I}$ and $\tilde{\mathbf{U}}'\mathbf{K}\tilde{\mathbf{U}} = \mathbf{0}$. Thus, \mathbf{K} does not penalize γ_{unpen} (Wand, 2000; Fahrmeir et al., 2004).

The columns of $\tilde{\mathbf{U}}$ are then a basis of the nullspace of \mathbf{K} and $\tilde{\mathbf{V}}$ can be obtained from the spectral decomposition of the prior precision matrix $\mathbf{K} = \tilde{\mathbf{\Gamma}}\mathbf{\Omega}^+\tilde{\mathbf{\Gamma}}'$ with $\mathbf{\Omega}^+$ the diagonal matrix of positive eigenvalues and $\tilde{\mathbf{\Gamma}}$ the corresponding matrix of orthonormal matrix of eigenvectors. Moreover, $\tilde{\mathbf{V}} = \mathbf{L}(\mathbf{L}'\mathbf{L})^{-1}$ where $\mathbf{L} = \tilde{\mathbf{\Gamma}}\mathbf{\Omega}^{+1/2}$. Thus, the model equation for the response in matrix notation is now

$$\mathbf{y} = \mathbf{E}^x\beta + \mathbf{Z}\gamma + \varepsilon = \mathbf{E}^x\beta + \mathbf{Z}(\tilde{\mathbf{V}}\gamma_{pen} + \tilde{\mathbf{U}}\gamma_{unpen}) + \varepsilon = \mathbf{E}^x\beta + \mathbf{V}\gamma_{pen} + \mathbf{U}\gamma_{unpen} + \varepsilon \quad (8)$$

with design matrices $\mathbf{V} = \mathbf{Z}\tilde{\mathbf{V}}$ and $\mathbf{U} = \mathbf{Z}\tilde{\mathbf{U}}$. Then, the dimensions of γ_{pen} equals the rank of the precision matrix \mathbf{K} and γ_{unpen} is the unpenalized part of dimension $d - r$.

We do the same for the observed spatial covariate \mathbf{x} , such that our joint Bayesian spatial+ model follows

$$\mathbf{x} = \beta_0^x\mathbf{1} + \mathbf{V}\gamma_{pen}^x + \mathbf{U}\gamma_{unpen}^x + \varepsilon^x \quad (9a)$$

$$\mathbf{y} = \beta_0\mathbf{1} + \beta\varepsilon^x + \mathbf{V}\gamma_{pen} + \mathbf{U}\gamma_{unpen} + \varepsilon \quad (9b)$$

where we generally assume the same penalty and design matrix for the thin plate regression

splines used to model both \mathbf{y} and \mathbf{x} .

The new likelihood of the data given the unknown parameter vector $\boldsymbol{\vartheta}$ is

$$\begin{aligned}\mathbf{y}|\mathbf{x}, \boldsymbol{\vartheta} &\sim N(\beta_0 \mathbf{1} + \beta \boldsymbol{\varepsilon}^x + \mathbf{V}\boldsymbol{\gamma}_{pen} + \mathbf{U}\boldsymbol{\gamma}_{unpen}, \sigma^2 \mathbf{I}) \\ \boldsymbol{\varepsilon}^x &= \mathbf{x} - \beta_0^x \mathbf{1} - \mathbf{V}\boldsymbol{\gamma}_{pen}^x - \mathbf{U}\boldsymbol{\gamma}_{unpen}^x \\ \mathbf{x}|\boldsymbol{\vartheta} &\sim N(\beta_0^x \mathbf{1} + \mathbf{V}\boldsymbol{\gamma}_{pen}^x + \mathbf{U}\boldsymbol{\gamma}_{unpen}^x, \sigma_x^2 \mathbf{I})\end{aligned}$$

where $\boldsymbol{\vartheta}$ is the vector of all model parameters. A marginalized version of the considered likelihood has been considered for example in Marra and Wood (2011), and later in Wood (2016). Other authors have used the partially improper density in Equation (5) to obtain the full conditionals of $\boldsymbol{\gamma}|\tau^2$ and $\boldsymbol{\gamma}_x|\tau_x^2$. However, in our experience, the latter leads to less stable results (see Appendix B) and the marginalized version converged extremely slowly compared to the current version, possibly because the resulting additive structure in the covariance, which is also weighted by two distinct smoothing parameters, is generally more difficult to estimate.

3.3 Prior hierarchy

The vector $\boldsymbol{\gamma}_{pen}$ follows a proper i.i.d. normal prior $\boldsymbol{\gamma}_{pen}|\tau^2 \sim N(0, \tau^2 \mathbf{I})$ and $\boldsymbol{\gamma}_{unpen}$ is the unpenalized part of dimension $d - r$ with zero precision matrix yielding a flat prior. In this way, $1/\tau^2$ can be interpreted as the precision of the deviation from the null space. Similarly to the response, $\boldsymbol{\gamma}_{pen}^x$ follows a proper i.i.d. normal prior $\boldsymbol{\gamma}_{pen}^x|\tau_x^2 \sim N(0, \tau_x^2 \mathbf{I})$ and $\boldsymbol{\gamma}_{unpen}^x$ is the unpenalized part of dimension with a flat prior.

Unless stated otherwise, the scale parameters (e.g., σ and σ_x) follow a non-informative and proper prior distribution $U(0, 100)$ (Gelman, 2006). We consider two adjusted Bayesian models, that differ in the way the priors for τ^2 and τ_x^2 are specified. The reformulation in Equation (9a) allows the proper construction of a hyperprior for τ^2 and τ_x^2 (Wand, 2000; Fahrmeir et al., 2004). The two alternative we consider are presented in Section 3.3.1 and

Section 3.3.2.

3.3.1 Independent smoothness prior

In the first version of the Bayesian spatial+, we use the prior proposed by Klein et al. (2015). Consider the vectors \mathbf{z}_i^d , $i = 1, \dots, n$, such that $\mathbf{Z} = (\mathbf{z}_1^d, \dots, \mathbf{z}_n^d)'$. Then, $\mathbf{z}_i^{d'} \boldsymbol{\gamma} | \tau^2 \sim N(0, \tau^2 \mathbf{z}_i^{d'} \mathbf{Z}^- \mathbf{z}_i^d)$, where the generalized inverse \mathbf{Z}^- is derived from the spectral decomposition $\mathbf{Z}^- = (\tilde{\mathbf{\Gamma}} \mathbf{\Omega}_d^+ \tilde{\mathbf{\Gamma}}')^-$. Klein et al. (2015) derive a prior

$$\begin{aligned} \tau^2 &\sim Weibull(0.5, \zeta), \\ \tau_x^2 &\sim Weibull(0.5, \zeta_x) \end{aligned}$$

where ζ can be chosen such that

$$P(|\mathbf{z}_i^d \boldsymbol{\gamma}| \leq c, \forall \mathbf{s} \in \mathcal{S}) \geq 1 - \alpha, \quad (10)$$

with $\alpha \in (0, 1)$ and $c > 0$, and ζ_y can be chosen such that

$$P(|\mathbf{z}_i^d \boldsymbol{\gamma}^x| \leq c_x, \forall \mathbf{s} \in \mathcal{S}) \geq 1 - \alpha_x \quad (11)$$

where $\alpha_x \in (0, 1)$ and $c_x > 0$. We follow the suggestion of Klein et al. (2015) to use $c = c_x = 3$ and we consider different values of α and α_x .

Essentially, this prior, which follows the penalized complexity principles in Simpson et al. (2017) shrinks the model towards a base model with $\tau^2 \rightarrow 0$ and $\tau_x^2 \rightarrow 0$, and thus $\beta_{pen} \rightarrow 0$ and $\beta_{pen}^x \rightarrow 0$, unless the data indicates the appropriateness of the more complex model. In general, by imposing high smoothing for the spatial effect of the response, we avoid that the spatial effect of the response operates at a too small scale and potentially partially explains the observed spatial covariate. From Section 2.2, we also know smoothing is not as problematic in spatial+ as in an unadjusted spatial model. By also imposing some smoothness

on $f^x(\cdot)$, we can prevent that there is no variation left in the residuals $\varepsilon^x(\cdot)$ after fitting the spatial model, although in general we can impose less smoothing for the covariate compared to the response by allowing larger values of α_x .

3.3.2 Joint smoothness prior

Independently penalizing the two spatial effects for τ^2 and τ_x^2 may help preserve some confounding bias. It has been argued that spatial confounding arises when the spatial scale of the response (the smoothness) becomes smaller than the covariate's, as it is able to explain more than the covariate, as shortly mentioned in Section 3.3.1. If one can guarantee $f(\cdot)$ is a smoother of $f^x(\cdot)$, then $\varepsilon_x = x(\cdot) - \beta_0^x - f^x(\cdot)$ removes the large scale dependence between $x(\cdot)$ and $y(\cdot)$, leaving only smaller spatial scale behavior in ε_x , which is not confounded with $f(\cdot)$ (see Paciorek, 2010; Guan et al., 2022; Mäkinen et al., 2022). Similarly to the case with independent priors, we consider a prior

$$\tau^2 \sim \text{Weibull}(0.5, \zeta), \quad (12)$$

but now explicitly model

$$\tau_x^2 = \tau^2 \sigma_x^2 / \sigma^2 + \xi, \quad (13)$$

$$\xi \sim p(\cdot), \quad (14)$$

or alternatively,

$$\tau_x = \tau \sigma_x / \sigma + \xi, \quad (15)$$

$$\xi \sim p(\cdot) \quad (16)$$

where $p(\cdot)$ is a continuous distribution with positive support. This implies that $f(\cdot)$ exhibits more smoothness than $f^x(\cdot)$ since $\lambda = \sigma^2 / \tau^2 > \lambda_x = \sigma_x^2 / \tau_x^2$ (Nychka, 2000). This structure

imposes restrictions on the prior for the smoothness rather than directly on the posterior distribution of the spline coefficients. Thus, overall, along with (weakly) informative priors for τ^2 that shrink towards high smoothness of the response’s spatial effect, we consider this approach to modeling the correlation between the covariates and the spatial effects less problematic than imposing restrictions on the posterior, such as in restricted spatial regression (Reich et al., 2006; Khan and Calder, 2020). Indeed, if the data reveals that the prior is to some degree inappropriate, this should be revealed in the posterior distribution, of course while still respecting the support of the prior.

From Section 2.2, we know that strong bias due to oversmoothing of the response is a worry only for the standard spatial model, given that λ and λ_x satisfy $\lambda\lambda_x = o(n^{-1})$. However, a potential risk here is that if the observed covariate already has little non-spatial variation, imposing that the corresponding spatial effect to be less smooth than the unobserved’s covariate might deteriorate the performance of the model further. However, this should be counterbalanced by the prior for τ^2 with strong shrinkage towards zero, and thus towards high smoothness, such that imposing less smoothness of the observed covariate should not be problematic. Additionally, this can be mediated by the prior chosen for ξ . For example, a prior with shrinkage towards zero could guarantee that the spatial process on the response is smoother of the covariate’s, while still guaranteeing that the latter is not undersmoothed such that there is no variation left in the residuals. In this paper, we use non-informative priors for $p(\cdot)$ (see Appendix C). Concretely, we test $IG(0.001, 0.001)$ in Equation (14) and $U(0, 100)$ in Equation(16).

The complete prior hierarchy is shown together in Appendix A.

3.4 Sampling

The Bayesian spatial+ is implemented with **R-stan** (Stan Development Team, 2023) which employs the No U-Turn Sampler (NUTS, Hoffman et al., 2014) for an efficient exploration of the posterior. NUTS takes advantage of available gradient information and updates all

parameters are in one block. Using one single block update is a perk of **R-stan**, which becomes helpful in models with confounded parameters, as sampling these parameters together is more efficient than sampling them independently (see e.g. Rue and Held, 2005). Due to spatial confounding and potential feedback effects (as discussed in Section 3.5), it is advisable to update all spatial effects and the regression coefficients β as a single MCMC block as this promotes better convergence.

3.5 Feedback effects

Zigler et al. (2013) state that one salient feature of unifying distinct modeling stages with Bayesian joint estimation is that doing so allows “feedback” between the stages, which may lead to bias of the estimated coefficients. In causal inference, the view is that the first stage is meant to approximate the design stage of a randomized study and that this should be done without any access to the outcome to ensure objective design decisions that are entirely separate from analysis decisions (see, e.g. Rubin, 2008). In a joint Bayesian model, quantities in a model for the outcome contribute information to posterior distributions of quantities in the model for the exposure. However, in many applications the set-up is different from a randomized trial, such that this interdependence is not conceptually problematic. Zigler et al. (2013) indicates as the problematic scenarios those in which the covariate-outcome surface cannot be expressed as a simple rescaling of the covariate-treatment surface. Given that we have at least two additive spatial effects on the response level, our current model would fit this setting. We argue that updating all spatial components and respective coefficients β in one block, combined with informative priors, should mitigate any impacts of “feedback” on inference and convergence, while allowing us to use a conventional Bayesian model that fully propagates uncertainty and allows us to build joint priors for the smoothness in both model equations. For example, the joint prior for smoothness in Section 3.3.2 should reduce identification issues between the two spatial effects, since the prior requires that the (spatial effect of the) response is a smoother of the (spatial effect of the) covariate.

Some solutions have been suggested to avoid feedback. There are concerns that the “cutting feedback” approach in Zigler et al. (2013) would disrespect rules of probability. In the simulation study, we instead compare the Bayesian spatial+ to the plug-in two-step approach from Stephens et al. (2023), that uses the posterior mean of the model parameter from the first stage on the second stage and as been suggested as a solution to “feedback” effects that leads to less bias in a Bayesian framework. This solution ultimately behaves similarly to the frequentist spatial+.

4 Extensions to multiple covariates

In the case of K spatially aligned covariates, the methodology follows naturally when we penalize the smoothness of the spatial effects independently. Concretely, we aim to remove the spatial component of each covariate and use each of the covariates’ corresponding residuals in the model for the response. When considering a joint prior for the smoothness of the observed and unobserved covariates, the extension is also simple if we model separately the smoothness of the observed spatial covariates. That is, for the q -th, $q = 1, \dots, K$, spatially-indexed observed covariate $x_q(\mathbf{s})$, we impose a similar prior as before but with covariate-specific variance parameter τ_{xq} in the prior of the penalized components of the thin plate regression splines. Similar to Equation (13), we impose

$$\tau_{xq}^2 = (\tau^2 \sigma_{xq}^2) / \sigma^2 + \xi_q$$

with covariate-specific and independent ξ_q distributed as in Equation (14). It follows similarly for σ_{xq}^2 . Alternatively, one could also adapt the specifications in Equations (15) and (16). Thus, the smoothness of the spatial effect of each observed covariate is imposed to be higher than the response’s, but the smoothness of the different observed covariates are independent. This is also, we believe, the most logical extension, as we are not investigating potential confounding between observed covariates, and suggest using typical solutions from linear

regression models in those cases (see Chapter 3 of Fahrmeir and Lang, 2001, for more details).

5 Simulation

In this section we perform a number of simulation studies. We distinguish between a data generating and an analysis model (DGM and DAM, respectively). The former is a model used to generate the data. The latter is the model used to analyze the observed data. We assume $y(\mathbf{s}_i)$ is observed at location $\mathbf{s}_i \in \mathbb{R}^2$ for $i = 1, \dots, n$.

We consider three simulation studies. In Simulation study 1, we revisit the simulation study from Dupont et al. (2022), and consider additional combinations for the spatial range of the unobserved and observed covariates. We consider a situation with model misspecification where the spatial indexed variables in the DGM are generated using Gaussian processes. In Simulation study 2, we study the impact of increasing the non-spatial information in the observed covariate, with the expectation that bias is reduced and coverage improved, not only for spatial+ but for all models. In Simulation Study 3, we examine the effects of reducing the correlation between observed and unobserved covariates. The details and results of this study can be found in Appendix D as the outcomes align with our expectations, namely, that lower correlation leads to reduced confounding.

In each simulation study, we consider the: (1) bias of β , (2) standard error of β , (3) mean squared error of β , (4) coverage of the true β . For the frequentist spatial+, similarly to Dupont et al. (2022), we simply use the output from `mgcv` for the standard error of β , since inference uncertainty is not discussed in further detail in Dupont et al. (2022). We denote these the naive standard errors.

5.1 Simulation Study 1

We reproduce the simulation study from Dupont et al. (2022), with some variations detailed below. By nature the original example has low non-spatial information, and for a more

complete perception of how spatial+ for different amount of non-spatial information see Simulation study 2.

5.1.1 Data generating model

We generate 50 independent replicates of covariate and response data observed at $n \in \{200, 1000\}$ random locations in a 50×50 regular grid in the spatial domain $[0, 10] \times [0, 10] \subseteq \mathbb{R}^2$ as follows:

$$\begin{aligned} y(\mathbf{s}_i) &= 3x(\mathbf{s}_i) - (z(\mathbf{s}_i) + z'(\mathbf{s}_i)) + \varepsilon_i \\ x(\mathbf{s}_i) &= 0.5z(\mathbf{s}_i) + \varepsilon_i^x \end{aligned}$$

where $\varepsilon_i^x \sim N(0, 0.1^2)$ and $\varepsilon_i \sim N(0, 0.1^2)$. Let $\mathbf{z} = (z(\mathbf{s}_1), \dots, z(\mathbf{s}_n))'$ and $\mathbf{z}' = (z'(\mathbf{s}_1), \dots, z'(\mathbf{s}_n))'$ denote observations at the selected locations of the independently generated Gaussian spatial fields with exponential and spherical covariance structure, respective. Particularly, we consider the exponential covariance $C_{\text{exp}}(h) = \exp(-(h/R^{\text{exp}}))$ where R^{exp} relates to the spatial range and $C_{\text{sph}}(h) = -1 - 1.5h/R^{\text{sph}} + 0.5(h/R^{\text{sph}})^3$ for $h \leq R^{\text{sph}}$, $C_{\text{sph}}(h) = 0$ for $h > R^{\text{sph}}$ with R^{sph} which controls spatial range of the spherical fields, where h denotes the Euclidean distance between two observations. Particularly, we consider the pairs $(R^{\text{exp}}, R^{\text{sph}}) \in \{(5, 1), (2.7, 1.6), (0.6, 10)\}$. The original paper considered $(R^{\text{exp}}, R^{\text{sph}}) = (5, 1)$ implying that at a distance of approximately 15 and 1 the correlation drops to 0.05 for $z(\cdot)$ and $z'(\cdot)$, respectively. This implies a much larger range for the covariate than for the spatial effect of the response, but also that there is not much spatial variation in the covariate, since at a distance of 10 the observations still have a correlation of approximately 0.2. While this particular scenario is somewhat extreme, scenarios where the covariate has a larger spatial range than the unobserved covariate are realistic in applications, such as when considering climatic covariates that have large spatial autocorrelation range, such that the effects of unobserved covariates operating at a finer spatial scale are realistic. The spatial correlations implied

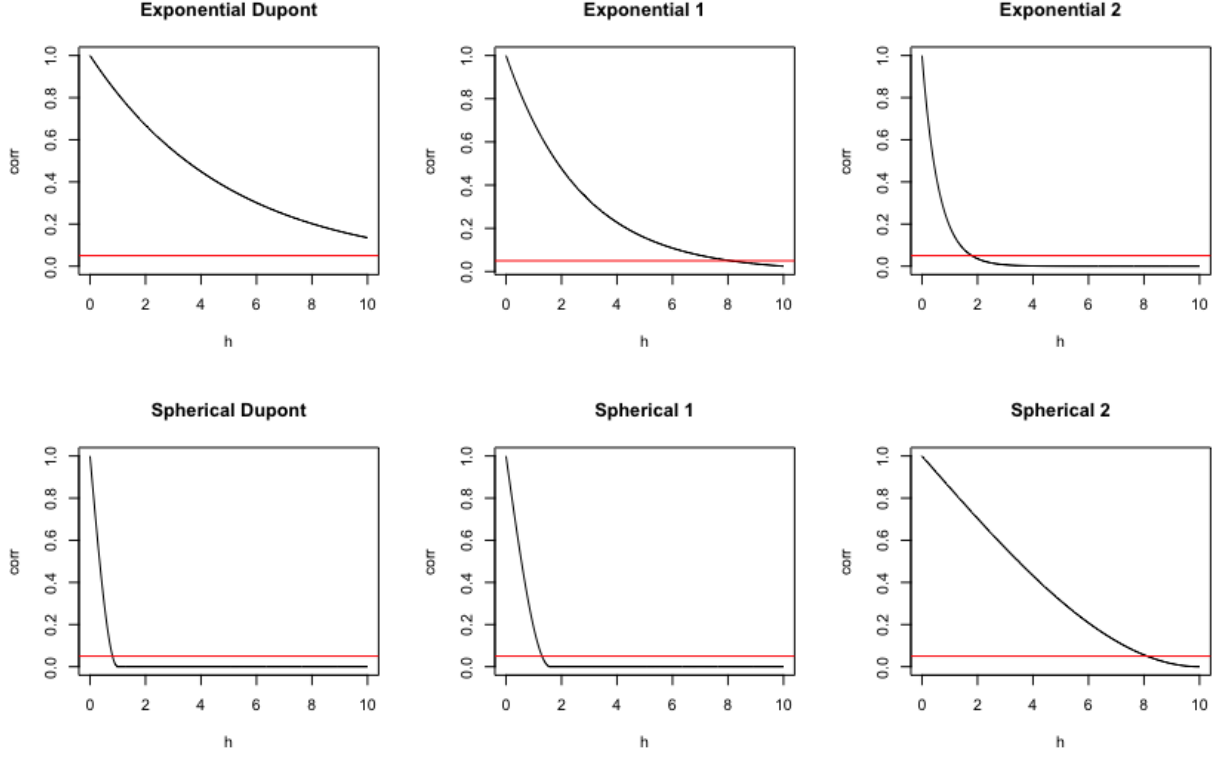


Figure 1: Spatial correlation as a function of the distance h in $[0, 10] \times [0, 10]$ for the spherical and exponential correlation function. Indices 1 and 2 indicate scenarios $(R^{\text{exp}}, R^{\text{sph}}) = (2.7, 1.6)$ and $(R^{\text{exp}}, R^{\text{sph}}) = (0.6, 10)$. The Dupont case corresponds to $(R^{\text{exp}}, R^{\text{sph}}) = (5, 1)$ from Dupont et al. (2022). The red line shows a correlation of 0.05.

by $(R^{\text{exp}}, R^{\text{sph}}) \in \{(5, 1), (2.7, 1.6), (0.6, 10)\}$ as a function of the distance h are shown in Figure 1.

In Dupont et al. (2022) the authors replace the sampled Gaussian fields by the fitted values of a spatial thin plate regression spline fitted to them. Here we use the sampled values directly. Hence, we consider the case of a misspecified DAM. The correlation between the observed and unobserved covariates implied by the three data generating processes is 0.71.

5.1.2 Data analysis model

Throughout the paper, we consider three possible approaches to modeling the relationship between $y(\mathbf{s})$ and $\mathbf{x}^{\text{obs}}(\mathbf{s})$: (1) a non-spatial model, (2) a “traditional”/standard spatial

model, and (3) an spatial model accounting for spatial confounding. Although the data generating process is spatial and one would not generally expect the non-spatial model to be a good competitor, it is included here as some literature in spatial confounding seems to suggest that the non-spatial model would lead to unbiased estimates of β (Briz-Redón, 2023, e.g.). We consider nine models in total. A frequentist non-spatial model (frequentist ns), standard spatial model (frequentist), and adjusted spatial model (frequentist spatial+). Moreover, we consider the Bayesian counterparts. A Bayesian non-spatial model (bayesian ns), a standard spatial models (bayesian), and four adjusted spatial models (bayesian+ and bayesian+ joint, as in Section 3.2, the gSTEM from Thaden and Kneib (2018) in Appendix E), and Bayesian spatial+ based on Stephens et al. (2023)). The method from Stephens et al. (2023) follows a plug-in two-step approach, where we use the posterior mean of β from the first stage is used on the second stage. Unsurprisingly, it behaves quite similarly to the frequentist spatial+ and we refrain from showing the results here, which are already extensive and it would not add any additional relevant information.

We opt for the priors in Equations (15) and (16) in the joint Bayesian spatial+ since in general the prior on the standard deviation performed slightly better than in the prior on the variance (see Section C). The scale-dependent Weibull priors are used for all spatial models. In Bayesian spatial+, we use $\alpha = 0.01$ as this always led to better results and spatial+ is less sensitive to smoothing. For the spatial models, $\alpha = 0.1$ is used, and thus we impose less shrinkage towards high smoothness, which leads to better results, as the spatial model is particularly sensitive to smoothing. This agrees with the general conclusion in Dupont et al. (2022) that the spatial model, without adjustment, is more sensitive to smoothing.

We consider samples sizes $n = 200, 1000$, with corresponding number of $k = 80, 300$ basis functions, respectively. A pragmatic approach to choose k is to increase k if the estimated degrees of freedom for a thin plate regression spline exceeds some specified proportion of the basis dimension, namely about 80% (see Wood, 2003).

We run two chains for all Bayesian models, with 3000 iterations, including a warm-up of

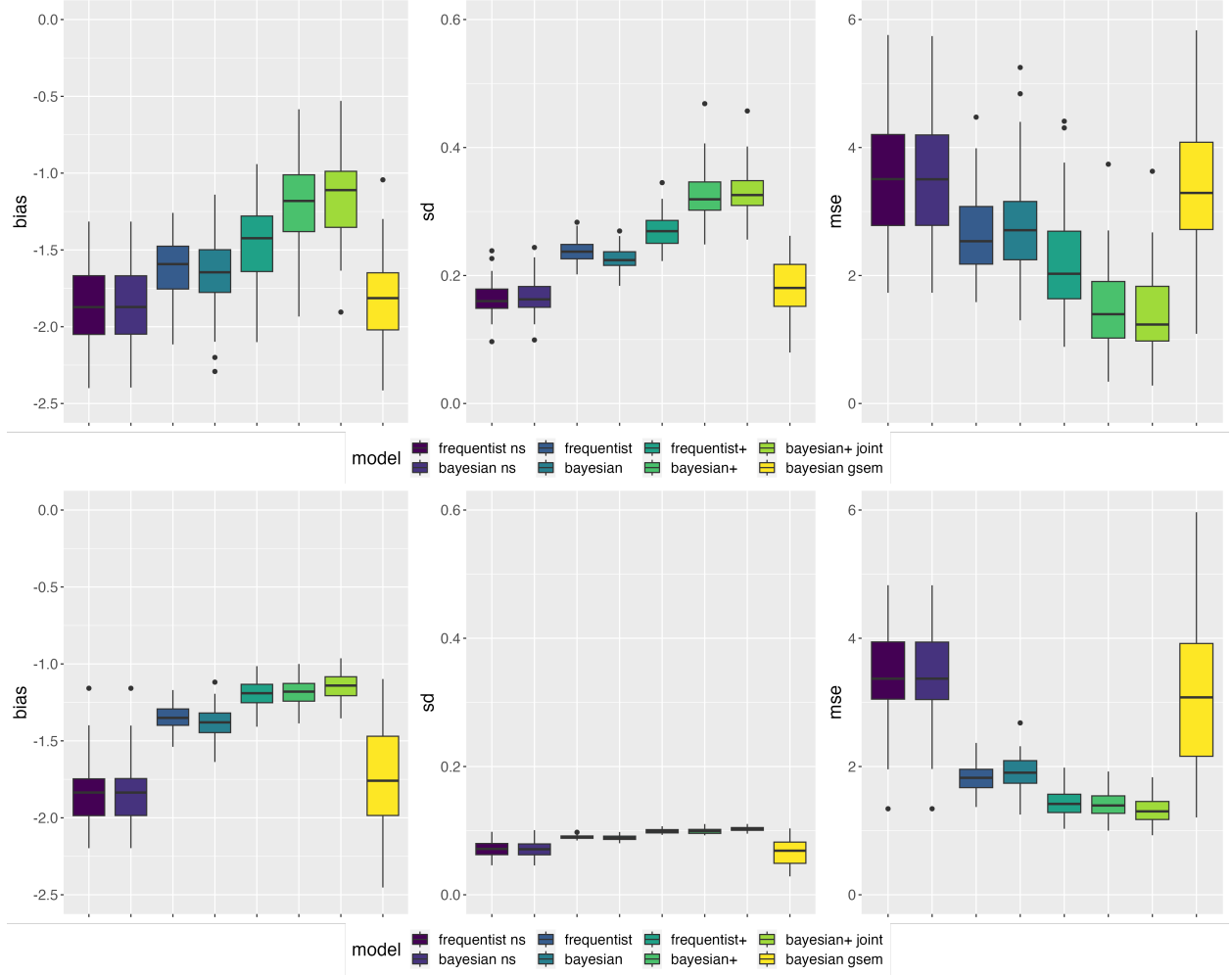


Figure 3: Results in Simulation study 1 for $n = 200$ (top) and $n = 1000$ (bottom) and $(R^{\text{exp}}, R^{\text{sph}}) = (2.7, 1.6)$. Left: bias; center: standard error (sd); right: mean squared error (mse).

variation in the residuals of the confounded covariate. A bias of zero is not achieved in a misspecified model. The frequentist spatial+ does not allow for uncertainty propagation from the first to the second stage of the model and, in the Bayesian version, the standard error of the β estimates is greater. This, combined with the smaller bias, leads to better cover rates for the bayesian+ variations in Table 1. This is sharp contrast with the results for all remaining models. When the sample size increases, the bias does not disappear, which combined with lower uncertainty, leads to a coverage of zero for all models. This is a general issue with the bias-variance trade-off and building confidence intervals around still biased

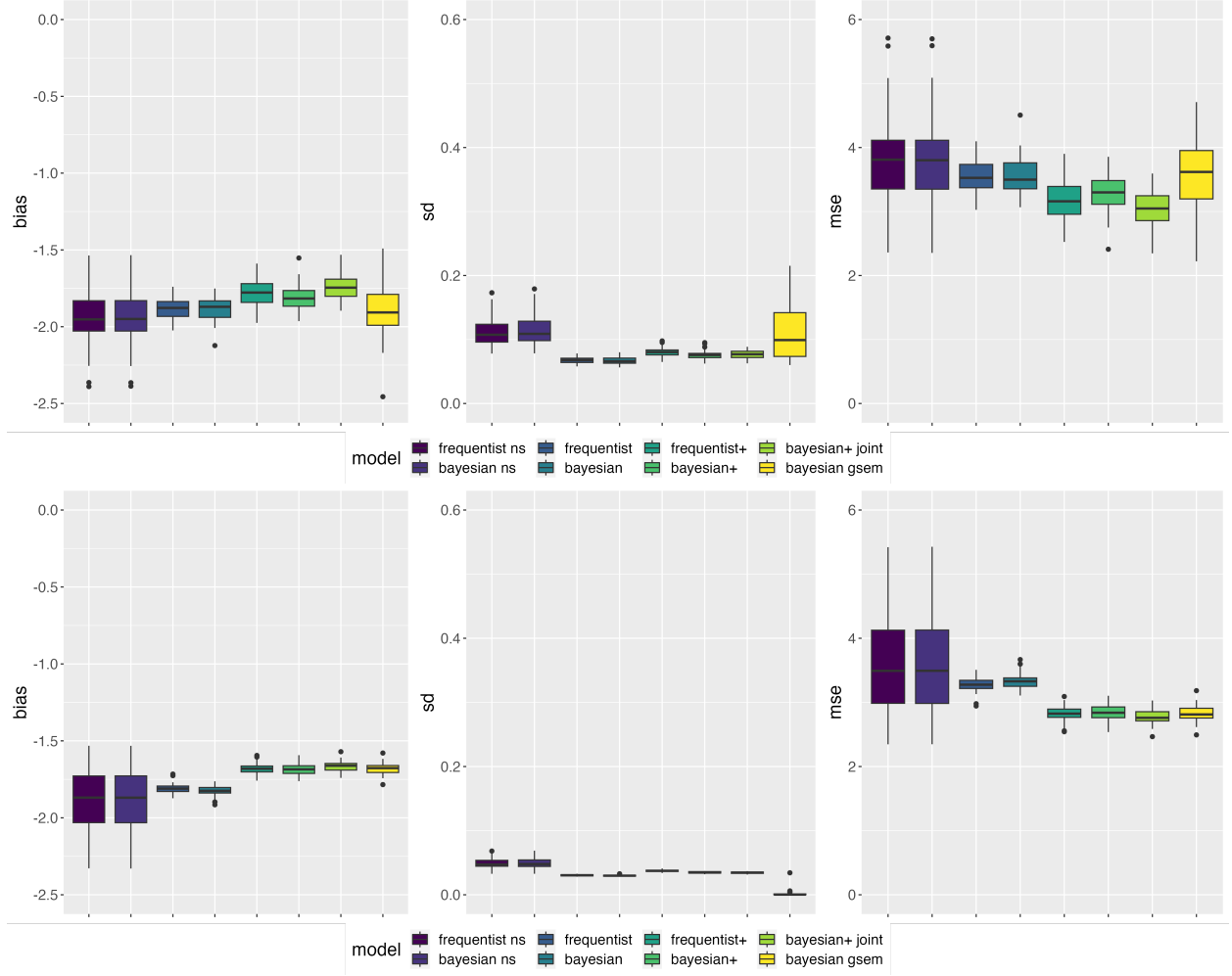


Figure 4: Results in Simulation study 1 for $n = 200$ (top) and $n = 1000$ (bottom) and $(R^{\text{exp}}, R^{\text{sph}}) = (0.6, 10)$. Left: bias; center: standard error (sd); right: mean squared error (mse).

estimates. Indeed, for any combination of priors used, we could not confirm the expectation in Section 2.2 that the bias converges faster than the standard deviation of β , although, ideally, the higher uncertainty in the bayesian+ estimates would compensate for the bias.

In Figures 3 and 4, we see the results for the remaining two scenarios. When the confounded components has a larger spatial scale, there is clear potential for bias reduction from using spatial and spatial+ model. For scenarios where the scale of the unobserved covariate is larger, implying confounding at a small scale, it becomes more difficult to reduce bias and all models ultimately lead to similar results.

$(R^{\text{exp}}, R^{\text{sph}}) = (5, 1)$								
	freq. ns	freq.	freq.+	bayes. ns	bayes.	bayes.+	bayes.+ joint	bayes. gstem
n=200	0	0.02	0.34	0	0	0.68	0.7	0
n=1000	0	0	0	0	0	0	0	0
$(R^{\text{exp}}, R^{\text{sph}}) = (2.7, 1.6)$								
n=200	0	0	0	0	0	0.04	0.06	0
n=1000	0	0	0	0	0	0	0	0
$(R^{\text{exp}}, R^{\text{sph}}) = (0.6, 10)$								
n=200	0	0	0	0	0	0	0	0
n=1000	0	0	0	0	0	0	0	0

Table 1: Coverage rates in Simulation study 1 for β based on 95% confidence/credible interval.

The issues with the coverage of β are even worse for these DGMs. This could be because in fact the confounded component in the example in Dupont et al. (2022) is at such a large spatial scale that spatial confounding is less of a problem.

Uncertainty is higher in the Bayesian versions of spatial+, especially for smaller sample sizes, suggesting that the frequentist version might underestimate it and the naive standard errors underestimate uncertainty. Using the joint model for the smoothnesses generally improves performance in all scenarios. For all DGMs, the non-spatial and gstem models perform considerably worse than the remaining models. The Bayesian standard spatial model can be unstable, such that is a greater advantage from using the adjusted spatial model in a Bayesian context.

5.2 Simulation study 2: non-spatial information in the observed covariate

In Simulation study 1, the amount of non-spatial information in the observed covariate is relatively low since $z(\cdot)$ has a variance of 1. In this simulation study, we test scenarios with $\sigma^x \in \{0.5, 1\}$, i.e., more non-spatial information than in Simulation study 1. This is expected to significantly affect results, since the spatial+ methodology strongly relies on the presence

of sufficient non-spatial variation in the observed covariates.

5.2.1 Data generating model

We use the same data generating model (DGM) as in Section 5.1 but now increase $\sigma^x = 0.5$.

5.2.2 Data analysis model

The data analysis model (DAM) model is exactly the same as in Section 5.1.

5.2.3 Results

The results for $\sigma_x = 0.5$ are shown in Figures 5, 6 and 7. Results are similar, but intensified, for $\sigma_x = 1$ and we refrain from displaying these. Intuitively, the bias, standard error and MSE of the regression coefficient are smaller when the observed covariate has more non-spatial information. This is true for all models. The coverage of the estimated β also changes drastically, also for $n = 1000$. Thus, the amount of non-spatial information in the covariate significantly affects the performance of all models. Particularly, when the observed covariate is less smooth, for $n = 200$ we can now see the benefits of using spatial+, while before, the improvement were smaller.

In Table 2, we compare the coverage rate when $(R^{\text{exp}}, R^{\text{sph}}) = (5, 1)$ for the different signal to noise ratios. Even with $\sigma_x = 1$, the coverage rates drop for higher sample sizes, with the exception of the Bayesian spatial and Bayesian spatial+ models. For $\sigma_x = 1$ the coverage of the Bayesian spatial+ slightly exceeds to nominal rate. This indicates that spatial+ generally requires considerable non-spatial information to reach the expected behavior that the bias converges faster than the standard deviation, under this specific DGM. Moreover, the Bayesian models demonstrate better properties by not having declining coverage with sample size. The Bayesian model with joint prior for smoothness is generally the best performing model.

In Table 3, we show additional scenarios for the remaining combinations of the spatial

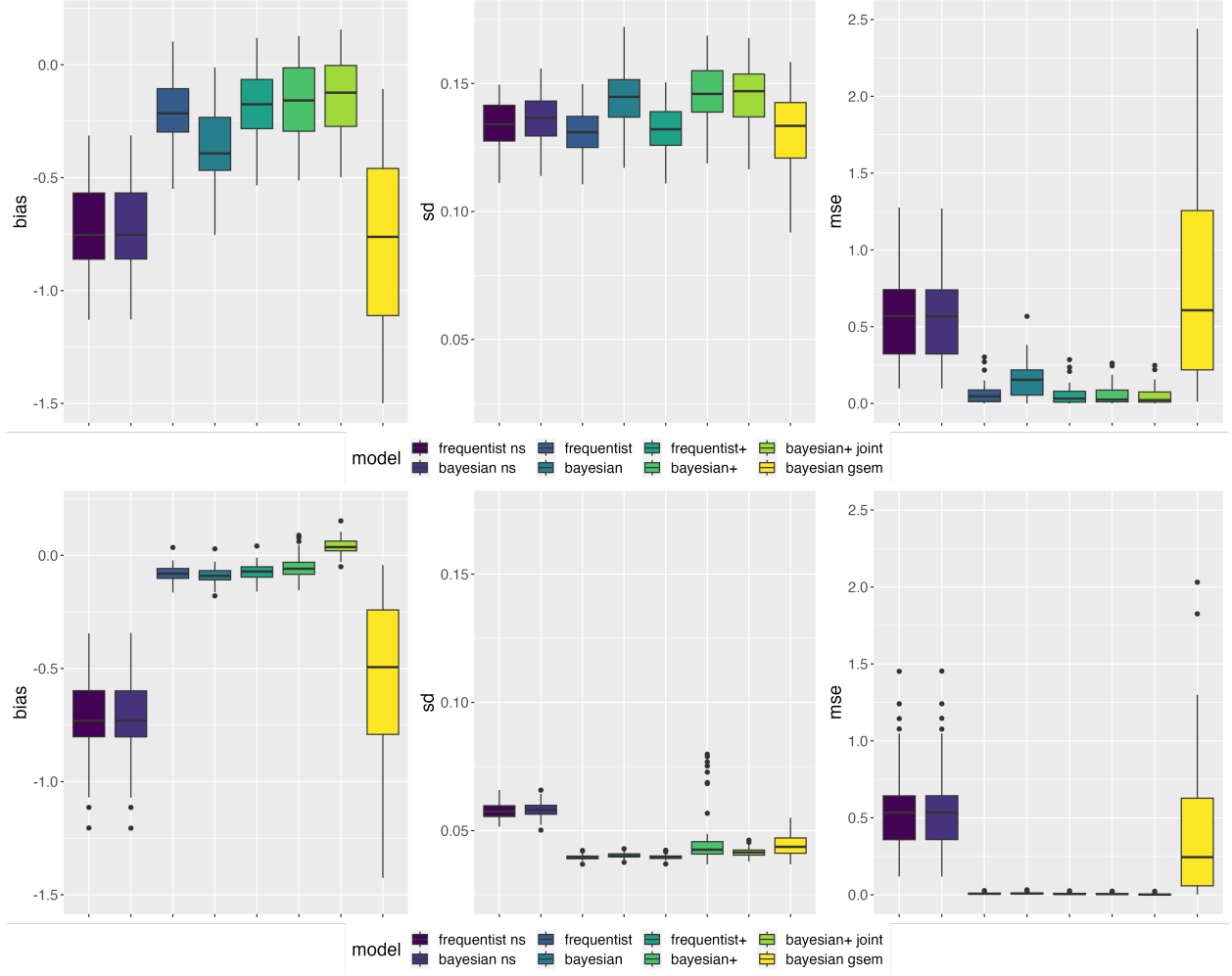


Figure 5: Results in Simulation study 2 for $n = 200$ (top) and $n = 1000$ (bottom) and $(R^{\text{exp}}, R^{\text{sph}}) = (5, 1)$. Left: bias; center: standard error (sd); right: mean squared error (mse).

range. For $(R^{\text{exp}}, R^{\text{sph}}) = (2.7, 1.6)$, the observed covariate has a smaller spatial range than in the example in Dupont et al. (2022). This seems to make it more difficult to eliminate confounding and with $\sigma_x = 1$ we still get an undesirable decrease in coverage rates for larger sample sizes. When $(R^{\text{exp}}, R^{\text{sph}}) = (0.6, 10)$ and confounding happens at low frequencies, we are once again unable to improve the coverage rate, even when having more non-spatial information in the observed covariate.

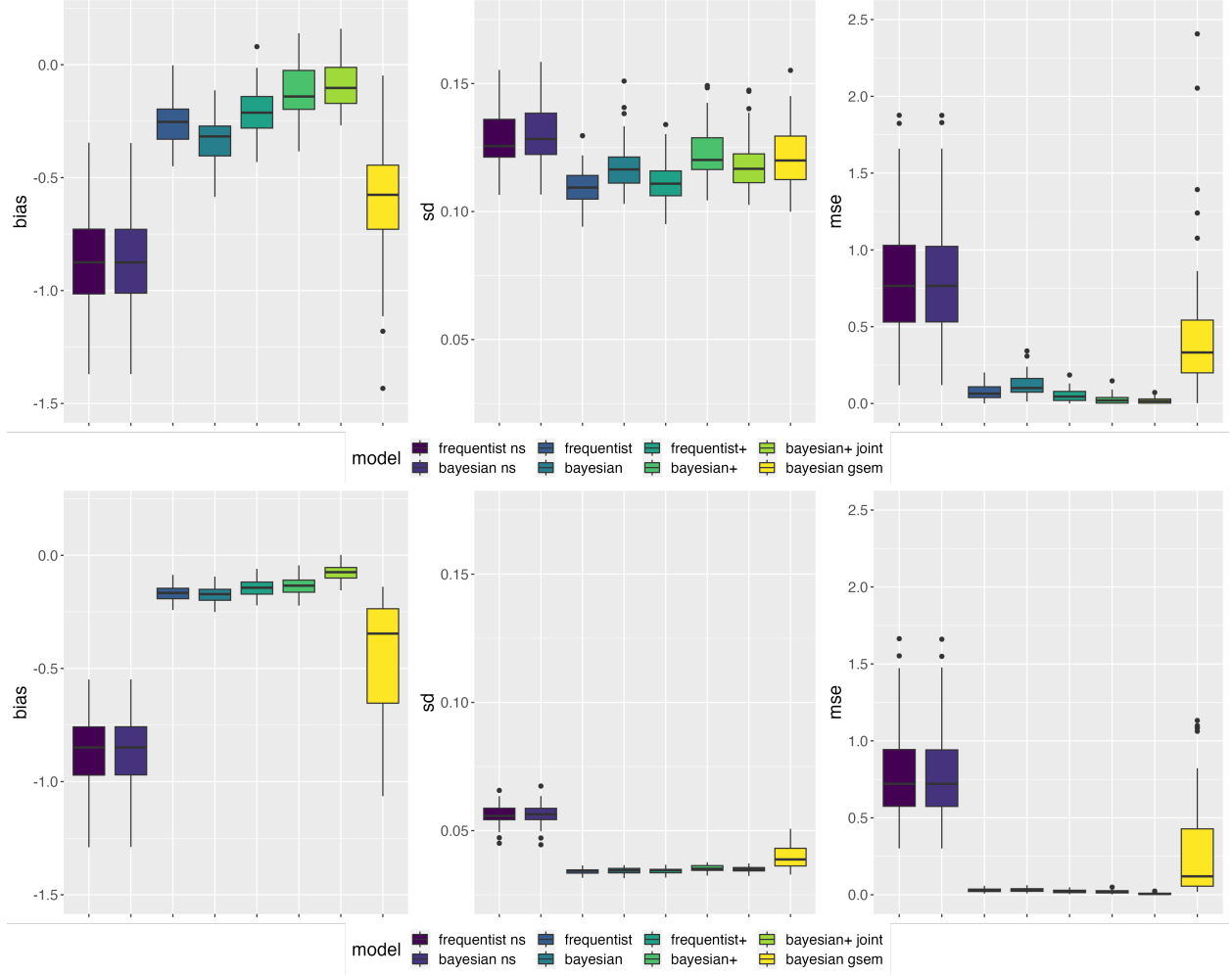


Figure 6: Results in Simulation study 2 for $n = 200$ (top) and $n = 1000$ (bottom) and $(R^{\text{exp}}, R^{\text{sph}}) = (2.7, 1.6)$. Left: bias; center: standard error (sd); right: mean squared error (mse).

5.3 General conclusions

The Bayesian spatial+ with joint prior for smoothness generally outperforms model competitors for the spatial scales considered. This is particularly visible in the coverage rates. It also generally leads to larger uncertainty estimates and, thus, better coverage in general, and for increasing sample size particularly.

The lower the non-spatial information in the observed covariate, the worse spatial+ performs, rendering the credibility intervals unreliable for scenarios with low non-spatial information (“noise-to-signal” ratio below 1). The Bayesian spatial+ and Bayesian models

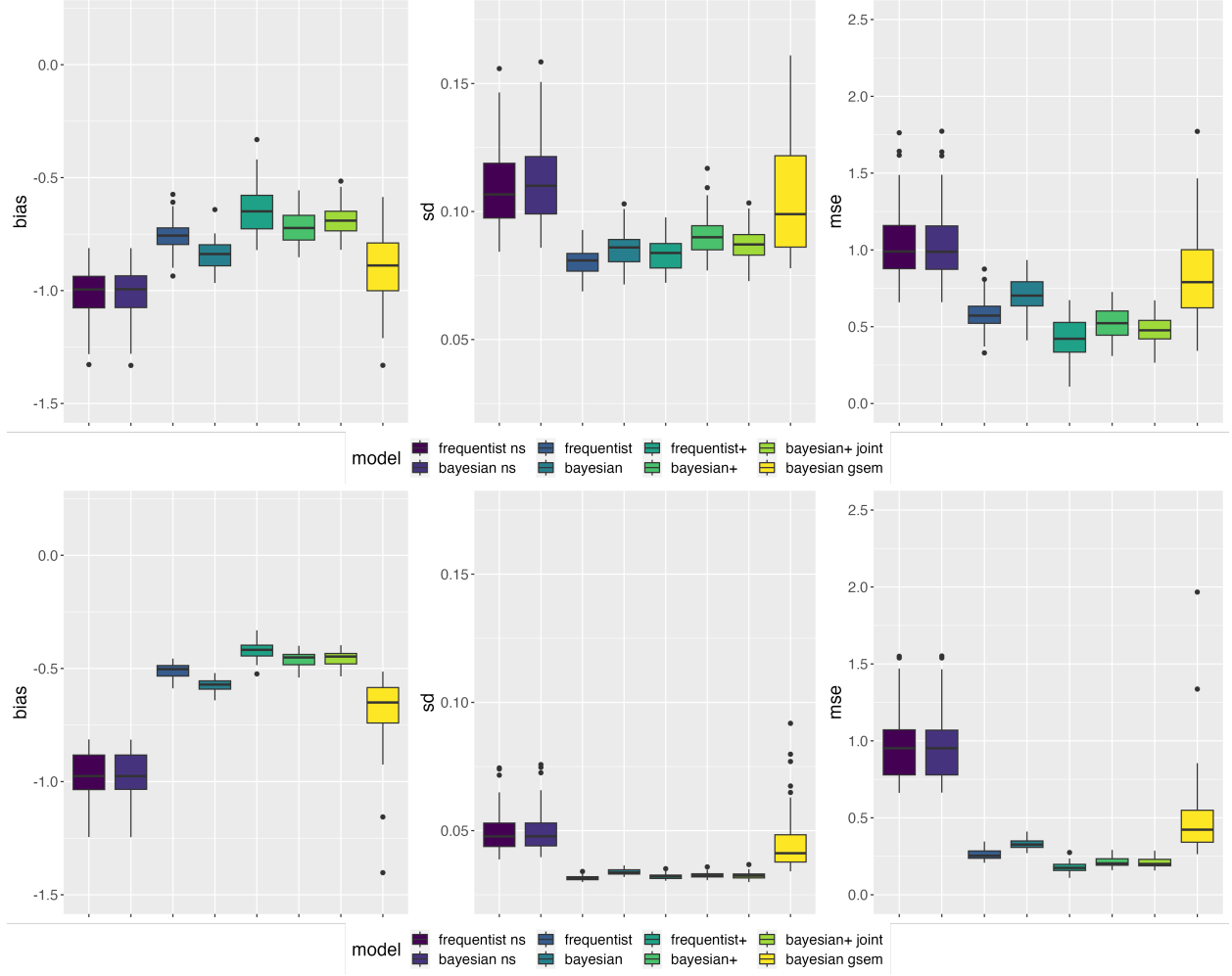


Figure 7: Results in Simulation study 2 for $n = 200$ (top) and $n = 1000$ (bottom) and $(R^{\text{exp}}, R^{\text{sph}}) = (1, 8)$. Left: bias; center: standard error (sd); right: mean squared error (mse).

in general seem more robust to this issue.

When confounding takes place at a larger scale we see stronger benefits from using spatial+ to disentangle the two effects. When this scale is small, all models struggle to disentangle confounding, even when the “noise-to-signal” is 1 (see Simulation study 2).

The spatial and spatial+ models are sensitive to the choice of α for the scale-dependent priors. However, after considering $\alpha \in \{0.01, 0.1, 0.2\}$, the spatial+ model mostly performed better with $\alpha = 0.01$ and the spatial model with $\alpha = 0.1$.

	$\sigma_x/\sigma_{fx} = 0.1$		$\sigma_x/\sigma_{fx} = 0.5$		$\sigma_x/\sigma_{fx} = 1$	
	n=200	n=1000	n=200	n=1000	n=200	n=1000
frequentist+	0.36	0	0.66	0.54	0.9	0.86
bayesian+	0.68	0	0.74	0.74	0.92	0.98
bayesian+ joint	0.7	0	0.76	0.9	0.92	0.96
frequentist	0.02	0	0.6	0.42	0.9	0.82
bayesian	0	0	0.34	0.38	0.76	0.76
bayesian gstem	0	0	0.06	0.04	0.2	0.24
frequentist ns	0	0	0.04	0	0.18	0.02
bayesian ns	0	0	0.04	0	0.18	0.02

Table 2: Coverage rates for β based on 95% confidence/credible interval. gstem corresponds to the model in Thaden and Kneib (2018).

	freq. ns	freq.	freq.+	bayes. ns	bayes.	bayes.+	bayes.+ joint	bayes. gstem
$(R^{\text{exp}}, R^{\text{sph}}) = (2.7, 1.6), \sigma_x = 0.5$								
n=200	0.02	0.38	0.42	0	0.16	0.86	0.9	0.04
n=1000	0	0	0	0	0	0.16	0.62	0
$(R^{\text{exp}}, R^{\text{sph}}) = (2.7, 1.6), \sigma_x = 1$								
n=200	0.06	0.7	0.7	0.06	0.6	0.92	0.92	0.24
n=1000	0	0.4	0.46	0	0.38	0.76	0.78	0.2
$(R^{\text{exp}}, R^{\text{sph}}) = (0.6, 10), \sigma_x = 0.5$								
n=200	0	0	0	0	0	0	0	0
n=1000	0	0	0	0	0	0	0	0
$(R^{\text{exp}}, R^{\text{sph}}) = (0.6, 10), \sigma_x = 1$								
n=200	0	0	0	0	0	0	0	0
n=1000	0	0	0	0	0	0	0	0

Table 3: Coverage rates in Simulation study 2 for β based on 95% confidence/credible interval.

6 Application

We consider two real datasets and study the performance of non-spatial, spatial and adjusted spatial models for each dataset, in both the frequentist and Bayesian framework. In terms of the adjusted models, we also consider the frequentist model Section 3.1 of Thaden and Kneib (2018), besides the Bayesian version corresponding to Section 3.2 of the same paper. We expect the similar point estimates from both versions but different uncertainty. Unlike the original gSEM, which considered discrete spatial data and used binary indicator variables for

each spatial location, here we use thin plate regression splines in a continuous spatial data context. Moreover, we here only consider the “bayesian+ joint” from the Simulation studies, as it always outperformed the Bayesian model with independent priors for smoothness.

6.1 Application 1: precipitation in Germany

In this application, we study average daily precipitation in January 2016 in Germany and consider average daily temperature and elevation as covariates. Temperature, but especially elevation in Germany, typically have a large spatial autocorrelation range, such that the effects of unobserved covariates operating at a finer spatial scale are realistic. We consider 277 locations and exclude the highest point in Germany, as it significantly affects the results. Indeed, Germany is relatively flat throughout the domain with the exception of the south and the observation corresponding to the highest point, also located in the south, stands out in the dataset. All variables are standardized. Concerning the expected effects of the covariates considered, one would typically expect higher temperatures to be associated with less rain and higher elevations with more rain.

6.1.1 Results

Figure 8 shows the results of fitting a thin plate regression spline model to the covariates and response. About 61% of the variability in the response is explained by the TPRSs, and 79 and 78% for temperature and elevation, respectively. These would represent scenarios in terms of the “noise-to-signal” ratio in Simulation study 2 is between 0.1 and 0.5. The confidence/credible interval for temperature includes zero in both Bayesian and frequentist non-spatial models. Including a spatial effect in the model increases the magnitude of this effect in all models, and none of the confidence/credible intervals include zero. This indicates that the covariate might indeed have spatially confounded information (e.g., as opposed to age in Application 2). The adjusted frequentist spatial model leads to a relatively insignificant absolute decrease of the mean effect of temperature, while for the Bayesian version the

effect becomes even more negative. Thus, the Bayesian version is potentially better able to reduce bias. The gSEM behaves similarly to the spatial model in both settings. For elevation, none of the confidence/credible intervals include zero. Including spatial effects increases the mean coefficients quite noticeably. Particularly, the spatial+ leads to a large magnitude increase in both frequentist and Bayesian settings. Thus, not only does elevation seem to suffer from spatial confounding, but the spatial+ methodology seems more able to apply corrections, while for temperature only the Bayesian version seems to accrue some changes. Both the coefficients for temperature and for altitude have the expected sign in all spatial models. Uncertainty estimates for the bayesian+ joint are larger than for other any other model, corroborating the idea that the Bayesian model does a better job at propagating uncertainty.

Ultimately, not only plotting the spatial structure of the covariates and looking at the mean estimates of the regression coefficients for all models, but also looking at the UQ associated with these coefficients might help understanding whether we are under a scenario where the adjusted model contributes to the estimation of the effects.

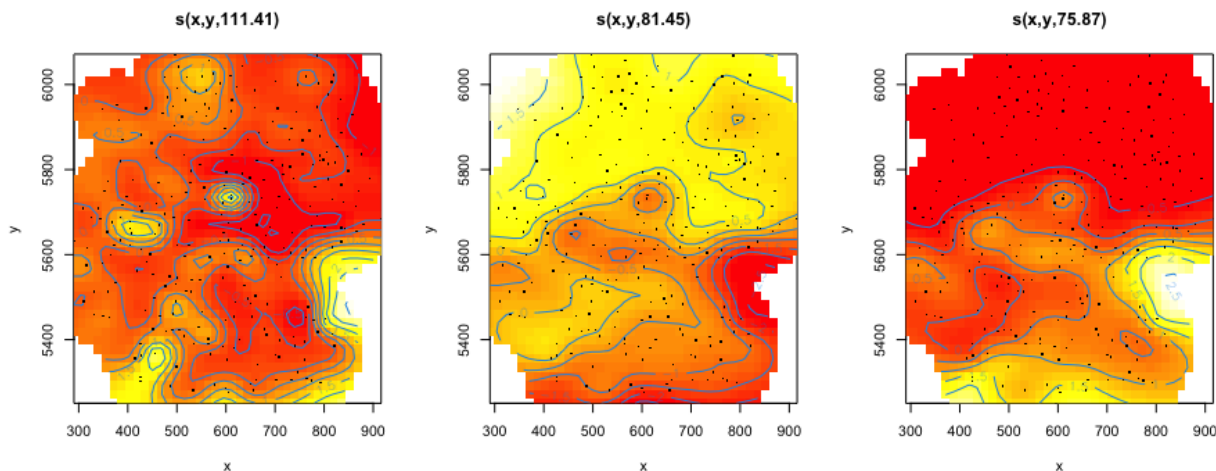


Figure 8: Output of thin plate regression splines applied to precipitation (left), temperature (center), elevation (right) using `mgcv`. $s(x, y, df)$ represents the spatial smooth, x and y the coordinates, and df the associated degrees of freedom.

	β_{temp}	sd_{temp}	$CI(\beta_{temp})$	β_{elev}	$sd(\beta_{elev})$	$CI(\beta_{elev})$
freq. ns	-0.09	0.16	[-0.39, 0.22]	0.49	0.16	[0.15, 0.77]
freq.	-0.45	0.12	[-0.68, -0.23]	0.74	0.12	[0.50, 0.97]
freq.+	-0.44	0.13	[-0.69, -0.16]	0.81	0.13	[0.55, 1.07]
freq. “gSEM”	-0.37	0.09	[-0.54, -0.19]	0.61	0.09	[0.43, 0.79]
bayes. ns	-0.09	0.16	[-0.41, 0.22]	0.45	0.16	[0.14, 0.76]
bayes.	-0.50	0.12	[-0.73, -0.27]	0.71	0.12	[0.47, 0.95]
bayes.+ joint	-0.57	0.17	[-0.9, -0.23]	0.85	0.17	[0.49, 1.18]
bayes. gSEM	-0.50	0.12	[-0.72, -0.27]	0.71	0.12	[0.46, 0.95]

Table 4: Mean estimated β_{temp} and β_{age} and corresponding standard deviation (sd) and credibility intervals (CI).

6.2 Application 2: tree coverage in Germany

In this section, we revisit the dataset in Dupont et al. (2022). Details on the original data are likewise available at Augustin et al. (2009). The dataset considers data on Spruce in 2013, corresponding to $n = 186$ observation locations in Germany. We study the effect of minimum temperature (temp) in May and tree age (age) on crown defoliation (defol) expressed as a ratio. High minimum temperature in May is indicative of a warmer year which, in turn, is likely to lead to higher levels of tree defoliation (measured later in the summer). All variables are standardized. Moreover, it is expected that older trees have more defoliation.

6.2.1 Results

In Figure 9 we show the resulting smooth function after fitting TPRSs to defoliation (left), age (center), temperature (right). Both defoliation and age are quite smooth and the spatial effect explains only a small percentage of the deviance in the data (less than 13%). Given the results in Section 5.2, this would lead us to expect less spatial confounding for age, which is confirmed by the results, where the coefficients are similar for all models, including the Bayesian versions. All coefficients being similar could also be similar to a scenario where the confounding takes place at a very small scale, similarly to the simulation studies, but this seems unlikely given the large spatial scale observed for all variables in Figure 9. In

Figure 9, the spatial structure of temperature seems considerably more complex and the thin plate regression spline explains about 76% of the deviance in the data. For temperature, the magnitude of the coefficients approximately doubles for the adjusted model compared to the unadjusted models. The non-spatial and spatial models also have very distinct coefficients for temperature. This indicates points towards the presence of spatial confounding. The results are consistent with Dupont et al. (2022).

Thus, it seems that age is dominated by non-spatial information that helps identifying its effect and correcting for spatial confounding is not as relevant. Temperature has more spatial variation that is confounded to a certain degree with the response.

Note that using a truly joint-type Bayesian model in gSEM, combined with a Bayesian framework, shrank the coefficient for temperature of the Bayesian gSEM to the Bayesian spatial model, when compared to the frequentist version. In a Bayesian context, only the Bayesian spatial+ provides significant estimates for temperature, with the Bayesian gSEM being quite close to being insignificant.

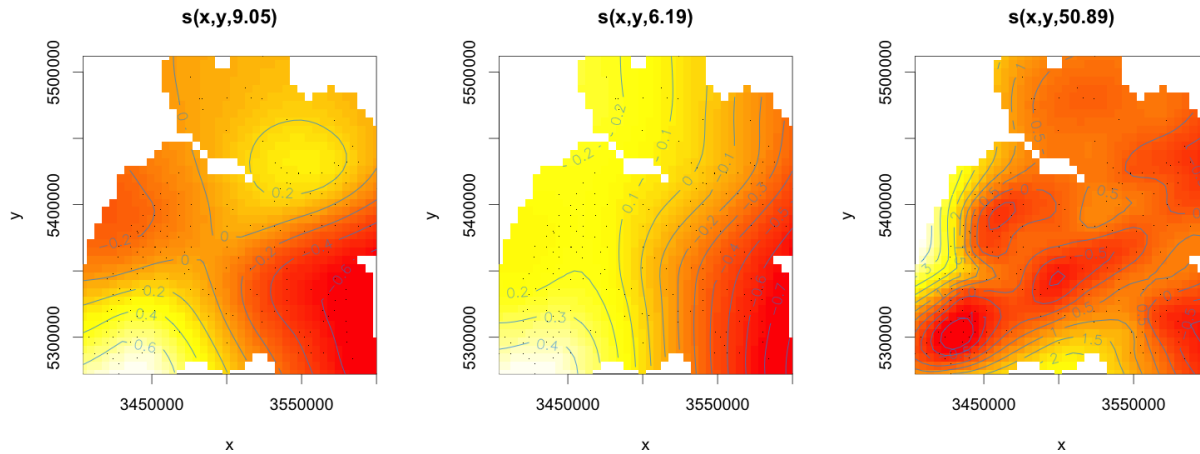


Figure 9: Output of thin plate regression splines applied to defoliation (left), age (center), temperature (right) using `mgcv`. $s(x, y, df)$ represents the spatial smooth, x and y the coordinates, and df the associated degrees of freedom.

	β_{age}	sd_{age}	$CI(\beta_{age})$	β_{temp}	$sd(\beta_{temp})$	$CI(\beta_{temp})$
freq. ns	0.70	0.05	[0.69, 0.71]	0.036	0.05	[0.03, 0.05]
freq.	0.68	0.05	[0.57, 0.78]	0.13	0.06	[0.01, 0.24]
freq. +	0.68	0.05	[0.57, 0.78]	0.27	0.10	[0.07, 0.46]
freq. "gSEM"	0.66	0.05	[0.56, 0.76]	0.27	0.10	[0.08, 0.046]
bayes. ns	0.70	0.05	[0.60, 0.81]	0.04	0.05	[-0.07, 0.14]
bayes.	0.68	0.05	[0.58, 0.79]	0.11	0.06	[-0.01, 0.22]
bayes. + joint	0.69	0.05	[0.58, 0.79]	0.27	0.10	[0.08, 0.47]
bayes. gSEM	0.68	0.05	[0.57, 0.78]	0.13	0.06	[0.00, 0.24]

Table 5: Mean estimated β_{temp} and β_{age} and corresponding standard deviation (sd) and confidence/credibility intervals (CI).

7 Discussion

In this paper, we bring the spatial+ methodology to a Bayesian framework. The advantages of implementing spatial+ in a Bayesian framework are in great part related to UQ. This includes uncertainty propagation in a two-stage model and the fact that UQ is generally more straightforward in a Bayesian context, and we cover a gap in the original manuscript, where inference beyond the mean is not explicitly detailed. Also relevant is the increased flexibility to impose restrictions on the prior according to known sources of spatial confounding, rather than directly on the posterior. Within a Bayesian framework, we develop a joint prior for the smoothness of all spatial effects. We explicitly address previous findings concerning the sources of spatial confounding, by developing a joint prior for the smoothness of all spatial effects that prevents that the spatial effect associated with the unobserved covariate is less smooth than the observed covariates', and thus that the spatial effect in the response operates at a smaller scale than the covariate's residuals in the outcome stage of spatial+ (Paciorek, 2010; Mäkinen et al., 2022).

The model is evaluated in simulation studies and applied in two applications. Overall, spatial+ is a helpful technique for scenarios where the confounded covariates have enough spatial information and the confounding does not take place at too small scales. The Bayesian spatial+ with joint prior for smoothness outperforms all competitors in terms of both bias

and uncertainty, although the differences are – as expected – more significant for UQ. The uncertainty estimates are larger in Bayesian models and the coverage is generally more reliable, especially for the Bayesian model with joint prior for smoothness, and for increasing sample sizes. When the confounding takes place at small scales, all models struggle in reducing bias. Spatial+ is crucially dependent on the amount of non-spatial information, such that initial checks are required before using it in real data applications. Bayesian plug-in approaches such as in Stephens et al. (2023) behave similarly to the frequentist spatial+ model, and are generally worse than the Bayesian counterpart, thus indicating that there are ways to control the negative impacts of the “feedback effects” of joint Bayesian models, without radically dropping the use of joint models.

Thus, overall, there are strong benefits to using spatial+ to reduce spatial confounding. The Bayesian version improves on the original version by giving us a proper UQ and reliable coverage intervals, conditional on having sufficient non-spatial information. Proper UQ also gives us more tools to detect identification issues in applications. The need of sufficient non-spatial information is inherent to the model and cannot be changed without completely rethinking of the model. However, our joint prior aids in this task, by also trying to capture small scale unconfounded spatial behavior in the residuals, giving us more tools to identify regression coefficients. Thus, this is a crucial feature that must be accounted for in potential future variations of our model. Finally, the requirement of separability between residuals and spatial effects limits extensions of spatial+ to non-Gaussian covariates.

Acknowledgements

We extend our gratitude to Thomas Kneib for helpful comments and discussions. Isa Marques acknowledges support by the Deutsche Forschungsgemeinschaft (DFG, German Research Foundation) through CRC 990 “Ecological and Socioeconomic Functions of Tropical Lowland Rainforest Transformation Systems”.

Conflicts of interest

The authors report no conflicts of interest.

References

- Augustin, N. H., Musio, M., von Wilpert, K., Kublin, E., Wood, S. N., and Schumacher, M. (2009). Modeling spatiotemporal forest health monitoring data. *Journal of the American Statistical Association*, 104(487):899–911.
- Briz-Redón, Á. (2023). On alleviating spatial confounding issues with the Bayesian Lasso. *Research Square preprint*, doi:10.21203/rs.3.rs-2498913/v1.
- Clayton, D. G., Bernardinelli, L., and Montomoli, C. (1993). Spatial correlation in ecological analysis. *International Journal of Epidemiology*, 22(6):1193–1202.
- Dupont, E., Wood, S. N., and Augustin, N. H. (2022). Spatial+: a novel approach to spatial confounding. *Biometrics*, 78(4):1279–1290.
- Engle, R. F., Granger, C. W., Rice, J., and Weiss, A. (1986). Semiparametric estimates of the relation between weather and electricity sales. *Journal of the American Statistical Association*, 81(394):310–320.
- Fahrmeir, L., Kneib, T., and Lang, S. (2004). Penalized structured additive regression for space-time data: a Bayesian perspective. *Statistica Sinica*, 14(3):731–761.
- Fahrmeir, L. and Lang, S. (2001). Bayesian semiparametric regression analysis of multicategorical time-space data. *Annals of the Institute of Statistical Mathematics*, 53:11–30.
- Gelman, A. (2006). Prior distributions for variance parameters in hierarchical models (comment on article by Browne and Draper). *Bayesian Analysis*, 1(3):515–534.

- Gelman, A., Carlin, J., Stern, H., and Rubin, D. (1992). Inference from iterative simulation using multiple sequences. *Statistical Science*, 7(4):457–511.
- Gelman, A. and Hill, J. (2006). *Data analysis using regression and multilevel/hierarchical models*. Cambridge University Press.
- Guan, Y., Page, G. L., Reich, B. J., Ventrucci, M., and Yang, S. (2022). A spectral adjustment for spatial confounding. *Biometrika*, 110(3):699–719.
- Hanks, E. M., Schliep, E. M., Hooten, M. B., and Hoeting, J. A. (2015). Restricted spatial regression in practice: geostatistical models, confounding, and robustness under model misspecification. *Environmetrics*, 26(4):243–254.
- Hoffman, M. D., Gelman, A., et al. (2014). The No-U-Turn sampler: adaptively setting path lengths in Hamiltonian Monte Carlo. *Journal of Machine Learning Research*, 15(1):1593–1623.
- Khan, K. and Berrett, C. (2023). Re-thinking spatial confounding in spatial linear mixed models. *arXiv preprint arXiv:2301.05743*.
- Khan, K. and Calder, C. A. (2020). Restricted spatial regression methods: implications for inference. *Journal of the American Statistical Association*, 117(537):482–494.
- Klein, N., Kneib, T., Lang, S., Sohn, A., et al. (2015). Bayesian structured additive distributional regression with an application to regional income inequality in germany. *The Annals of Applied Statistics*, 9(2):1024–1052.
- Mäkinen, J., Numminen, E., Niittynen, P., Luoto, M., and Vanhatalo, J. (2022). Spatial confounding in Bayesian species distribution modeling. *Ecography*, 2022(11):e06183.
- Marques, I. and Kneib, T. (2022). Discussion on “spatial+: A novel approach to spatial confounding” by Dupont, E., Wood, S. and Augustin, N. *Biometrics*.

- Marques, I., Kneib, T., and Klein, N. (2022). Mitigating spatial confounding by explicitly correlating Gaussian random fields. *Environmetrics*, 33(5):e2727.
- Marra, G. and Wood, S. N. (2011). Practical variable selection for generalized additive models. *Computational Statistics & Data Analysis*, 55(7):2372–2387.
- Nychka, D. W. (2000). Spatial-process estimates as smoothers. In Schimek, M. G., editor, *Smoothing and Regression: Approaches, Computation, and Application*. Wiley.
- Paciorek, C. J. (2010). The importance of scale for spatial-confounding bias and precision of spatial regression estimators. *Statistical Science*, 25(1):107–125.
- Page, G. L., Liu, Y., He, Z., and Sun, D. (2017). Estimation and prediction in the presence of spatial confounding for spatial linear models. *Scandinavian Journal of Statistics*, 44(3):780–797.
- Ramsay, T. (2002). Spline smoothing over difficult regions. *Journal of the Royal Statistical Society Series B: Statistical Methodology*, 64(2):307–319.
- Reich, B. J., Hodges, J. S., and Zadnik, V. (2006). Effects of residual smoothing on the posterior of the fixed effects in disease-mapping models. *Biometrics*, 62(4):1197–1206.
- Reich, B. J., Yang, S., and Guan, Y. (2022). Discussion on “spatial+: A novel approach to spatial confounding” by Dupont, E., Wood, S. and Augustin, N. *Biometrics*.
- Rubin, D. B. (2008). For objective causal inference, design trumps analysis. *Annals of Applied Statistics*, 2(3):808–840.
- Rue, H. and Held, L. (2005). *Gaussian Markov random fields: theory and applications*. Chapman & Hall/CRC, Boca Raton.
- Sangalli, L. M., Ramsay, J. O., and Ramsay, T. O. (2013). Spatial spline regression models. *Journal of the Royal Statistical Society Series B: Statistical Methodology*, 75(4):681–703.

- Schnell, P. M. and Papadogeorgou, G. (2020). Mitigating unobserved spatial confounding when estimating the effect of supermarket access on cardiovascular disease deaths. *The Annals of Applied Statistics*, 14(4):2069–2095.
- Simpson, D., Rue, H., Riebler, A., Martins, T. G., and Sørbye, S. H. (2017). Penalising model component complexity: a principled, practical approach to constructing priors. *Statistical Science*, 32(1):1–28.
- Stan Development Team (2023). Stan modeling language users guide and reference manual. <https://mc-stan.org>.
- Stephens, D. A., Nobre, W. S., Moodie, E. E., and Schmidt, A. M. (2023). Causal inference under mis-specification: adjustment based on the propensity score (with discussion). *Bayesian Analysis*, 18(2):639–694.
- Thaden, H. and Kneib, T. (2018). Structural equation models for dealing with spatial confounding. *The American Statistician*, 72(3):239–252.
- Ugarte, M., Adin, A., and Goicoa, T. (2017). One-dimensional, two-dimensional, and three dimensional B-splines to specify space–time interactions in Bayesian disease mapping: model fitting and model identifiability. *Spatial Statistics*, 22:451–468.
- Urdangarin, A., Goicoa, T., Kneib, T., and Ugarte, M. (2023). A one-step spatial+ approach to mitigate spatial confounding in multivariate spatial areal models. *arXiv preprint arXiv:2308.11260*.
- Urdangarin, A., Goicoa, T., and Ugarte, M. D. (2022). Evaluating recent methods to overcome spatial confounding. *Revista Matemática Complutense*, 36:333–360.
- Vehtari, A., Gelman, A., Simpson, D., Carpenter, B., and Bürkner, P.-C. (2021). Rank-normalization, folding, and localization: an improved R-hat for assessing convergence of MCMC (with discussion). *Bayesian Analysis*, 16(2):667–718.

- Wahba, G. (1984). Partial spline models for the semi-parametric estimation of several variables. In *Statistical Analysis of Time Series, Proceedings of the Japan US Joint Seminar*, pages 319–329.
- Wand, M. P. (2000). A comparison of regression spline smoothing procedures. *Computational Statistics*, 15:443–462.
- Wood, S. N. (2003). Thin plate regression splines. *Journal of the Royal Statistical Society: Series B (Statistical Methodology)*, 65(1):95–114.
- Wood, S. N. (2016). Just another Gibbs additive modeller: interfacing JAGS and mgcv. *Journal of Statistical Software*, 75(7):1–15.
- Zigler, C. M., Watts, K., Yeh, R. W., Wang, Y., Coull, B. A., and Dominici, F. (2013). Model feedback in Bayesian propensity score estimation. *Biometrics*, 69(1):263–273.
- Zimmerman, D. L. and Ver Hoef, J. M. (2021). On deconfounding spatial confounding in linear models. *The American Statistician*, 76(2):159–167.

A Complete prior hierarchy

Recall that $\boldsymbol{\vartheta}$ is the vector of unknown parameters. The likelihood of our model is $p(\mathbf{y}, \mathbf{x}|\boldsymbol{\vartheta}) = p(\mathbf{y}|\mathbf{x}, \boldsymbol{\vartheta})p(\mathbf{x}|\boldsymbol{\vartheta})$. The complete model hierarchy, with the smoothness prior from Section 3.3.2 is:

$$\begin{aligned}
\mathbf{y}|\mathbf{x}, \boldsymbol{\vartheta} &\sim N(\beta_0 \mathbf{1} + \beta \boldsymbol{\varepsilon}^x + \mathbf{V}\boldsymbol{\gamma}_{pen} + \mathbf{U}\boldsymbol{\gamma}_{unpen}, \sigma^2 \mathbf{I}) \\
\boldsymbol{\varepsilon}^x &= \mathbf{x} - \beta_0^x \mathbf{1} - \mathbf{V}\boldsymbol{\gamma}_{pen}^x - \mathbf{U}\boldsymbol{\gamma}_{unpen}^x \\
\mathbf{x}|\boldsymbol{\vartheta} &\sim N(\beta_0^x \mathbf{1} + \mathbf{V}\boldsymbol{\gamma}_{pen}^x + \mathbf{U}\boldsymbol{\gamma}_{unpen}^x, \sigma_x^2 \mathbf{I}) \\
\beta_0^x, \beta_0, \beta &\propto \text{flat} \\
\boldsymbol{\gamma}_{unpen}^x, \boldsymbol{\gamma}_{unpen} &\propto \text{flat} \\
\boldsymbol{\gamma}_{pen}^x | \tau_x^2 &\sim N(0, \tau_x^2 \mathbf{I}) \\
\boldsymbol{\gamma}_{pen} | \tau^2 &\sim N(0, \tau^2 \mathbf{I}) \\
\tau^2 &\sim Weibull(0.5, \zeta) \\
\tau_x &= (\tau \sigma_x) / \sigma + \xi \\
\xi, \sigma, \sigma_x &\sim U(0, 100)
\end{aligned}$$

As detailed in Appendix C, we opt for the priors in Equations (15) and (16) since in general the prior on the standard deviation performed slightly better. For the prior in Section 3.3.1, we have $\tau_x^2 \sim Weibull(0.5, \zeta_x)$ and ξ is non-existing.

B Impropriety of the prior of the basis of the splines

In Section 3, we reparametrize the model so that we can still perform inference given the impropriety of the prior in Equation (5). However, one can simply use the improper prior in Equation (5) in the full-conditional for $\boldsymbol{\gamma}$ and $\boldsymbol{\gamma}_x$, without the need of inverting the precision or calculating its determinant. However, our general experience was that inference was more

unstable, ultimately leading to a worse performance of the model. The results are shown in Figure 10.

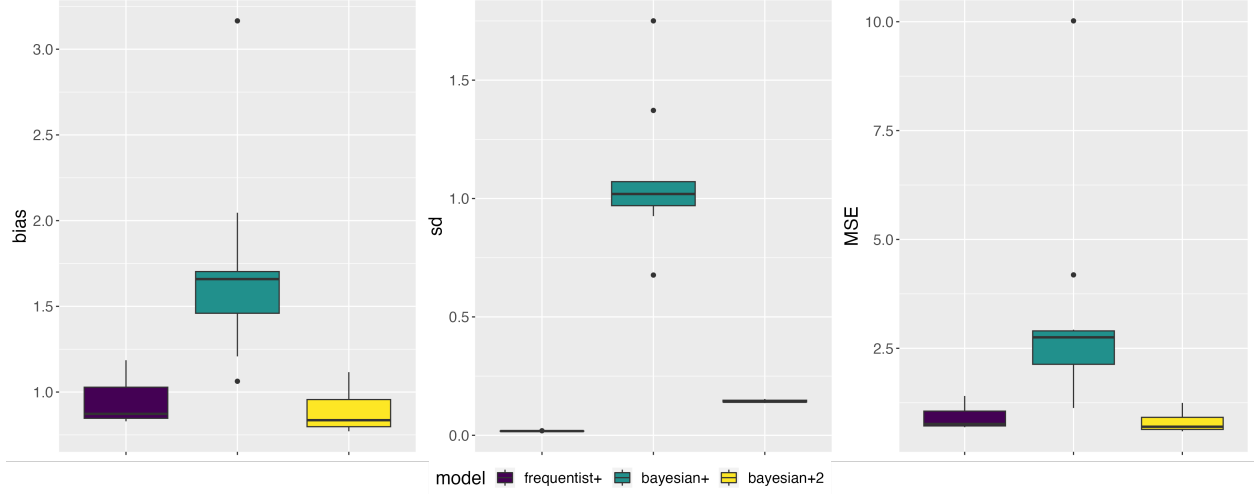


Figure 10: Comparing methods to deal with improper density. Bayesian+ 2 refers to the Bayesian spatial+ model which uses the a improper prior distribution γ and γ_x .

C Joint prior for smoothness

We considered different priors for $p(\cdot)$. Concretely, Option 1:

$$\tau_x^2 = (\tau^2 \sigma_x^2) / \sigma^2 + \xi \quad (17)$$

$$\xi \sim IG(0.001, 0.001) \quad (18)$$

or Option 2:

$$\tau_x = (\tau \sigma_x) / \sigma + \xi \quad (19)$$

$$\xi \sim U(0, 100) \quad (20)$$

where $p(\cdot)$ has positive support.

The results are show in Figure 11. The results show that the second prior is preferred in general.

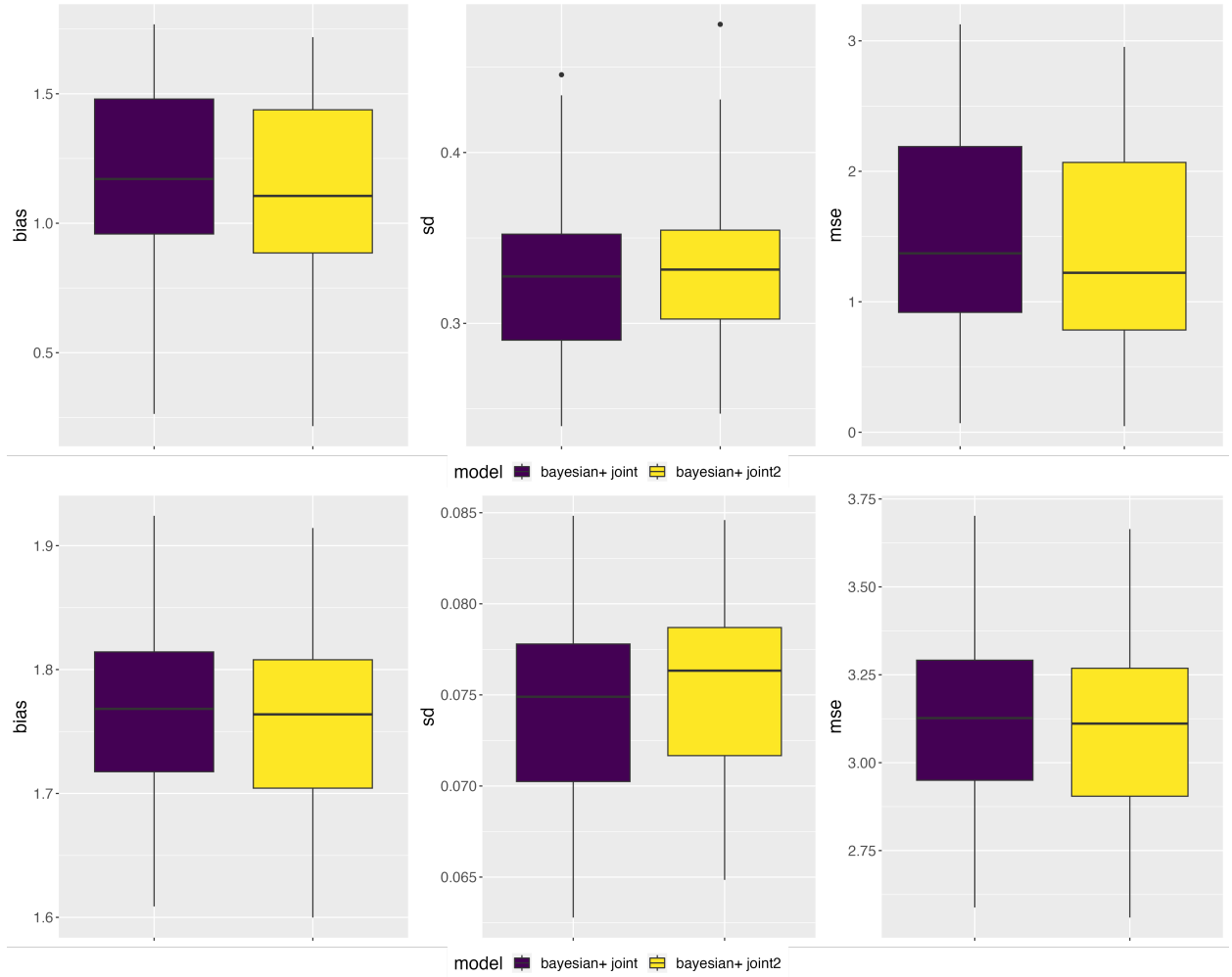


Figure 11: Comparing two priors ξ in joint prior for smoothness.

D Simulation study 3

D.1 Simulation study 3: correlation between observed and unobserved covariate

D.1.1 Data generating model

We use the same data DGM as in Section 5.1 but now reduce the correlation between observed and unobserved covariates. To achieve this without affecting the amount of spatial variation in the observed covariate, we distribute the variance in the unobserved covariate such that $f(\mathbf{s}) = \sqrt{0.5}z(\mathbf{s}) + \sqrt{1.5}z'(\mathbf{s})$ and the total variance of $f(\mathbf{s})$ is still 2, similarly to Sections 5.1 and 5.2.

D.1.2 Data analysis model

The DAM l is exactly the same as in Section 5.1.

D.1.3 Results

For lower correlation between the observed and unobserved covariates, the MSE and bias is smaller. This is rather intuitive and contradicts Khan and Berrett (2023). There is also an improvement in the coverage for the smaller sample sizes, but for larger sample sizes, the bias-variance trade-off once again wins over such that we generally get low coverage. In general, including a spatial component in the model leads to larger bias reduction when the observed covariate has higher smoothness. The Bayesian standard spatial model is, in general, less stable than the frequentist. When it comes to spatial+, the Bayesian joint spatial+ model outperforms the adjusted competitors or performs similarly well, and seems particular useful compared with the frequentist counterpart when the smoothness of the observed covariate is larger, but also when it is smaller. Thus, independently of the data generating process, imposing that the smoothness of the response is larger than the observed covariates in the DAM leads to better results.

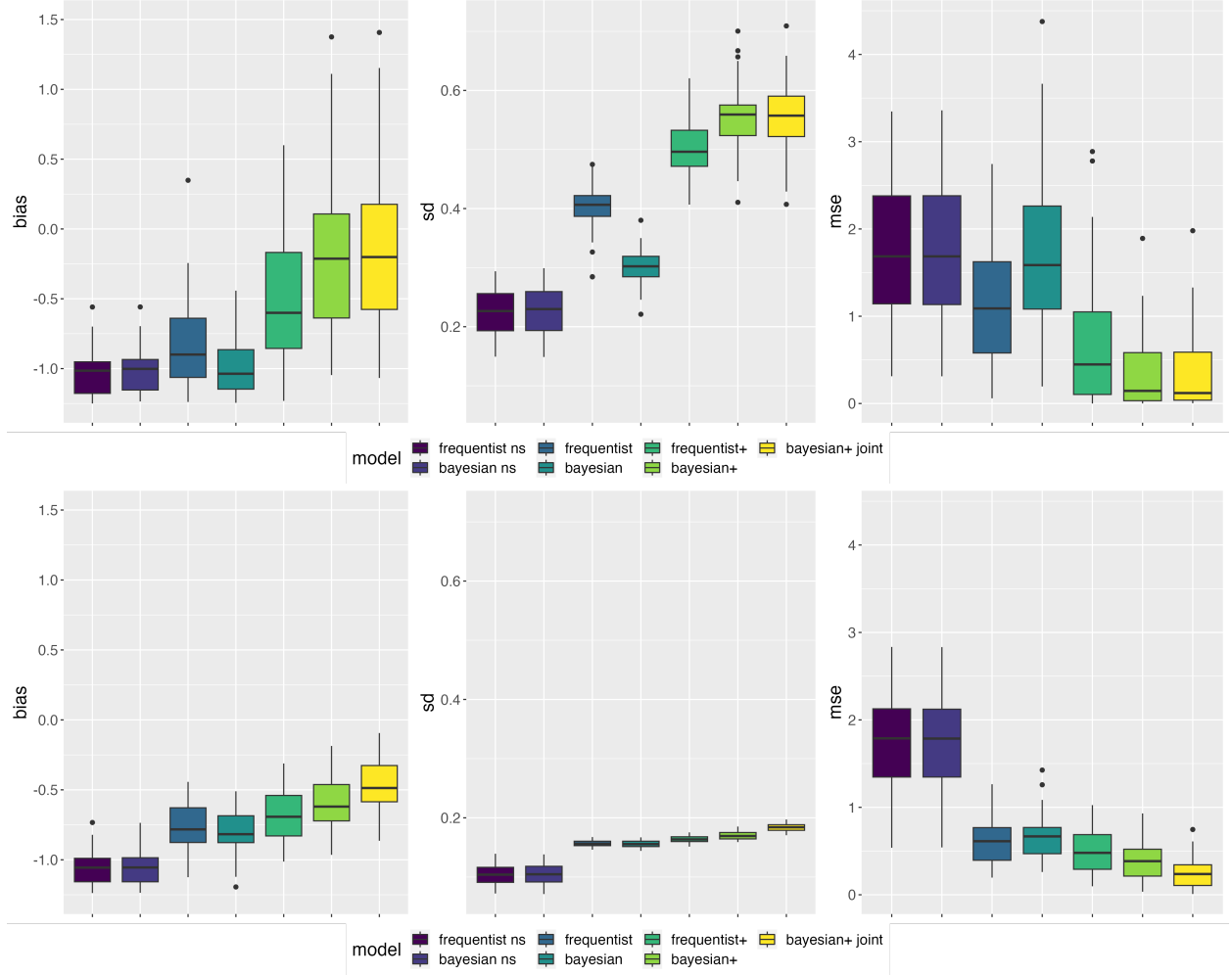


Figure 12: Results from Simulation Study 3 for $n = 200$ (top) and $n = 1000$ (bottom) and $(R^{\text{exp}}, R^{\text{sph}}) = (5, 1)$. Left: bias; center: standard error (sd); right: mean squared error (mse).

E Structural equation model

Thaden and Kneib (2018) proposed a structural equation model for alleviating spatial confounding. The manuscript focused on a frequentist version, but the authors also presented a Bayesian version with diffuse priors. Here we re-call the model structure and the priors we use for the Bayesian gSTEM in the simulation study and application. The frequentist version follows the model discussed in Section 3.1 of (Thaden and Kneib, 2018).

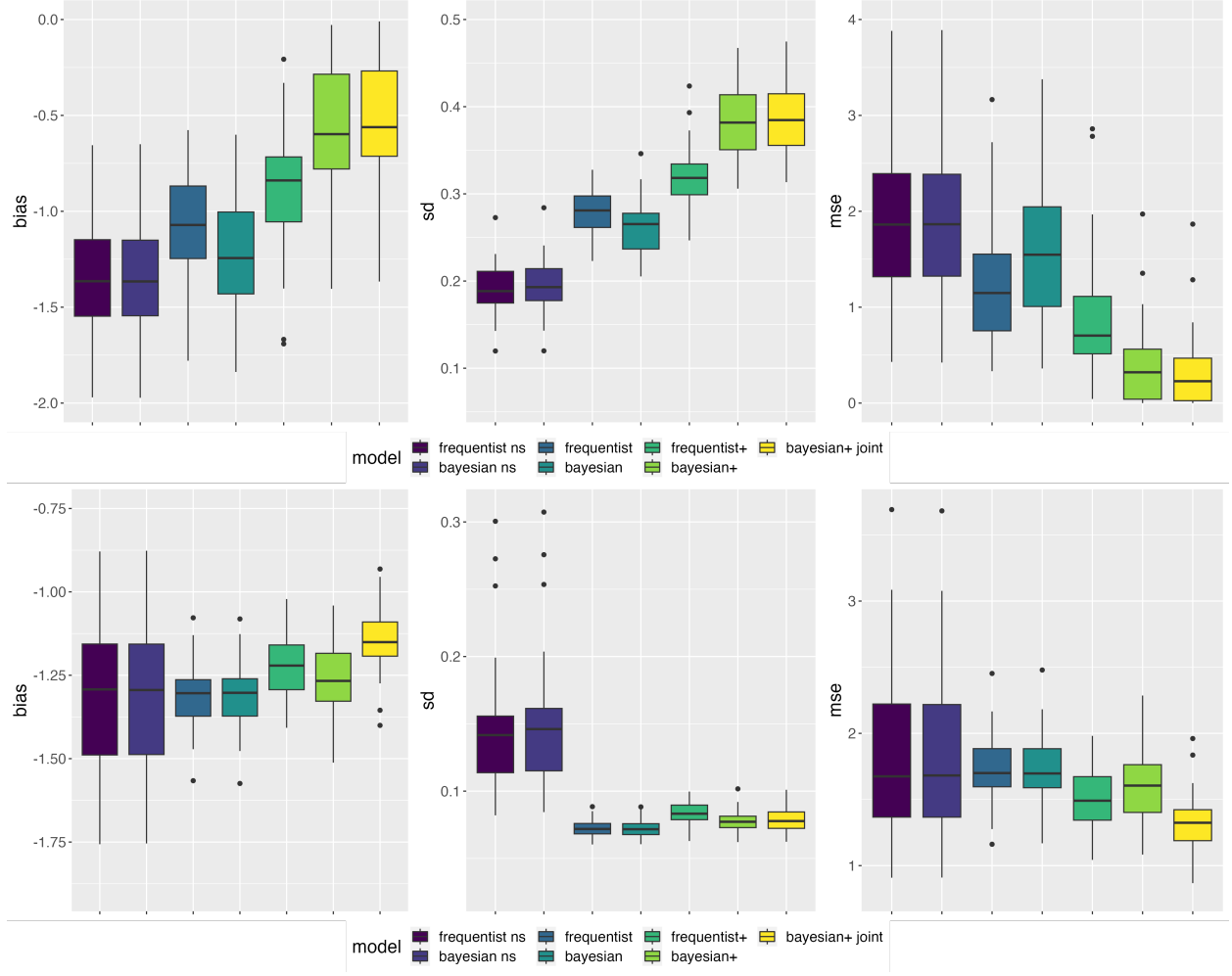


Figure 13: Results from Simulation Study 3 for $n = 200$ and $(R^{\text{exp}}, R^{\text{sph}}) = (2.7, 1.6)$, and $(R^{\text{exp}}, R^{\text{sph}}) = (0.6, 10)$. Top: $(R^{\text{exp}}, R^{\text{sph}}) = (2.7, 1.6)$. Bottom: $(R^{\text{exp}}, R^{\text{sph}}) = (1, 8)$. Left: bias; center: standard error (sd); right: mean squared error (mse).

$$\begin{aligned}
 \begin{bmatrix} \mathbf{x} \\ \mathbf{y} \end{bmatrix} &= \begin{bmatrix} 0 & 0 \\ \beta & 0 \end{bmatrix} \begin{bmatrix} \mathbf{x} \\ \mathbf{y} \end{bmatrix} + \begin{bmatrix} \mathbf{V}\gamma_{\text{pen}}^x \\ \mathbf{V}\gamma_{\text{pen}}^y \end{bmatrix} + \begin{bmatrix} \mathbf{U}\gamma_{\text{unpen}}^x \\ \mathbf{U}\gamma_{\text{unpen}}^y \end{bmatrix} + \begin{bmatrix} \boldsymbol{\varepsilon}^x \\ \boldsymbol{\varepsilon}^y \end{bmatrix} \\
 &= \mathbf{B} \begin{bmatrix} \mathbf{x} \\ \mathbf{y} \end{bmatrix} + \mathbf{V}\boldsymbol{\gamma}^{\text{pen}} + \mathbf{U}\boldsymbol{\gamma}^{\text{unpen}} + \boldsymbol{\varepsilon}.
 \end{aligned}$$

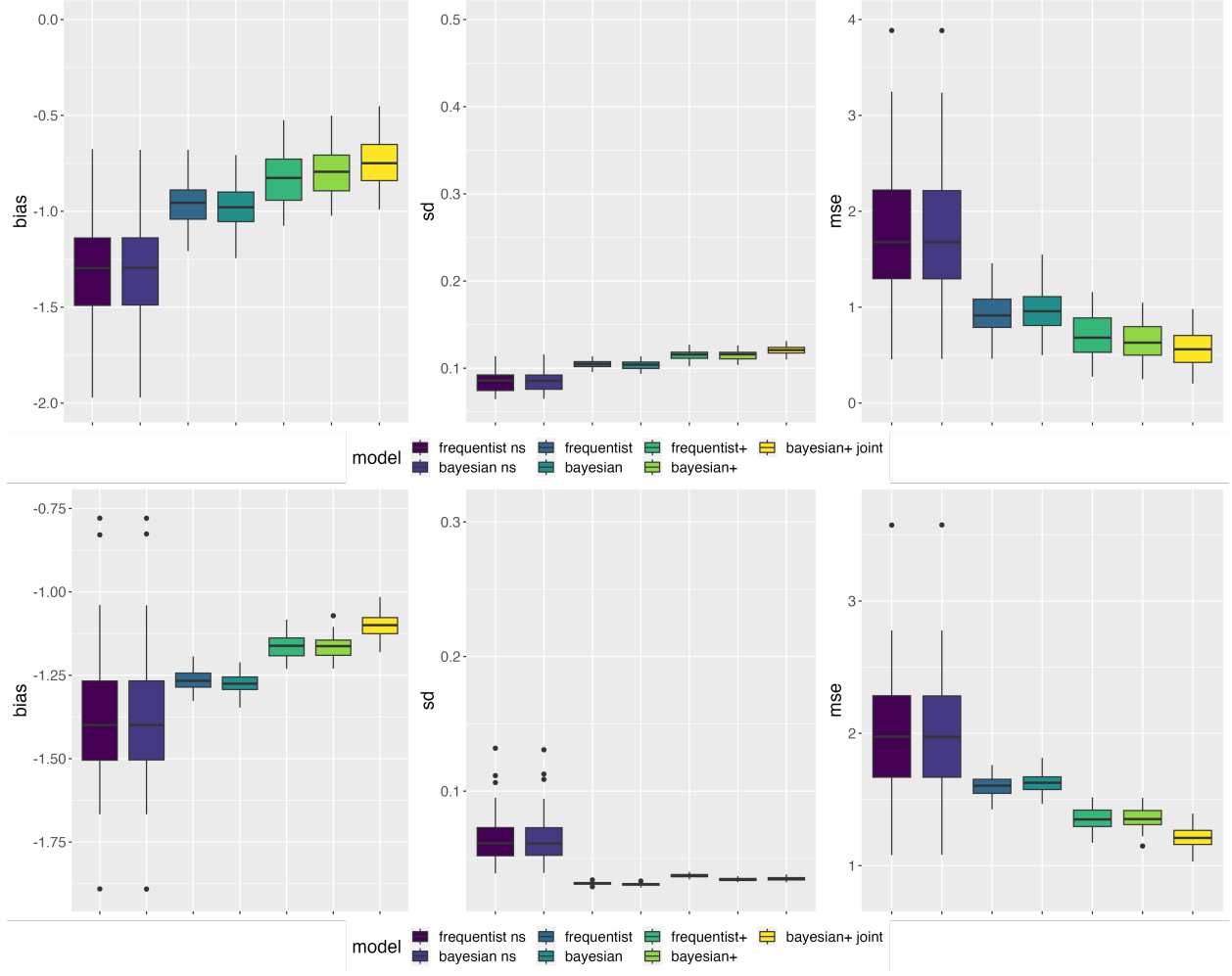


Figure 14: Results from Simulation Study 3 for $n = 1000$ and $(R^{\text{exp}}, R^{\text{sph}}) = (2.7, 1.6)$, and $(R^{\text{exp}}, R^{\text{sph}}) = (0.6, 10)$. Top: $(R^{\text{exp}}, R^{\text{sph}}) = (2.7, 1.6)$. Bottom: $(R^{\text{exp}}, R^{\text{sph}}) = (1, 8)$. Left: bias; center: standard error (sd); right: mean squared error (mse).

Let $\tilde{\mathbf{y}} = (\mathbf{x}', \mathbf{y}')'$ and $\Sigma = \begin{bmatrix} \sigma_x^2 & 0 \\ 0 & \sigma^2 \end{bmatrix} \otimes \mathbf{I}$. Then,

$$\tilde{\mathbf{y}} = (\mathbf{I} - \mathbf{B})^{-1} (\mathbf{V}\boldsymbol{\gamma}^{\text{pen}} + \mathbf{U}\boldsymbol{\gamma}^{\text{unpen}} + \boldsymbol{\varepsilon})$$

and

$$\tilde{\mathbf{y}} \sim N \left((\mathbf{I} - \mathbf{B})^{-1} (\mathbf{U}\boldsymbol{\gamma}^{\text{pen}} + \mathbf{V}\boldsymbol{\gamma}^{\text{unpen}}), (\mathbf{I} - \mathbf{B})^{-1} \Sigma ((\mathbf{I} - \mathbf{B})^{-1})' \right). \quad (21)$$

When compared to the model Thaden and Kneib (2018), denoted gSTEM, the only

$(R^{\text{exp}}, R^{\text{sph}}) = (5, 1)$								
	freq. ns	freq.	freq.+	bayes. ns	bayes.	bayes.+	bayes.+ joint	bayes gstem
n=200	0	0.6	0.66	0	0.34	0.74	0.76	0.06
n=1000	0	0.42	0.54	0	0.38	0.74	0.9	0.04
$(R^{\text{exp}}, R^{\text{sph}}) = (2.7, 1.6)$								
n=200	0.02	0.38	0.42	0	0.16	0.86	0.9	0.04
n=1000	0	0	0	0	0	0.16	0.62	0
$(R^{\text{exp}}, R^{\text{sph}}) = (0.6, 10)$								
n=200	0	0	0	0	0	0	0	
n=1000	0	0	0	0	0	0	0	

Table 6: Coverage rates for β on Simulation study 3 based on 95% confidence/credible interval.

difference lies on $\mathbf{\Gamma}^{\text{pen}}$ and $\mathbf{\Gamma}^{\text{unpen}}$ where the off diagonal elements are zero. We use this to compare the gSTEM to our Bayesian version of spatial+, with identical priors for gSTEM as in the prior hierarchy above.